Published in final edited form as:

J Immunol. 2015 August 1; 195(3): 1202–1217. doi:10.4049/jimmunol.1403013.

Ca^{2+} signaling but not store-operated Ca^{2+} entry (SOCE) is required for the function of macrophages and dendritic cells

Martin Vaeth[*], **Isabelle Zee**[*], **Axel R. Concepcion**[*], **Mate Maus**[*], **Patrick Shaw**[*], **Cynthia Portal-Celhay**[†], **Aleena Zahra**[†], **Lina Kozhaya**[*,†], **Carl Weidinger**[*], **Jennifer Philips**[*], **Derya Unutmaz**[*,†], and **Stefan Feske**[*]

[*]Department of Pathology, New York University School of Medicine, New York, NY 10016, USA

[†]Department of Medicine, New York University School of Medicine, New York, NY 10016, USA

Abstract

Store-operated Ca^{2+} entry (SOCE) through Ca^{2+} release-activated Ca^{2+} (CRAC) channels is essential for immunity to infection. CRAC channels are formed by ORAI1 proteins in the plasma membrane and activated by stromal interaction molecules 1 (STIM1) and STIM2 in the endoplasmic reticulum (ER). Mutations in *ORAI1* and *STIM1* genes that abolish SOCE cause severe immunodeficiency with recurrent infections due to impaired T cell function. SOCE has also been observed in cells of the innate immune system such as macrophages and dendritic cells (DC) and may provide Ca^{2+} signals required for their function. The specific role of SOCE in macrophage and DC function, and its contribution to innate immunity, however, is not well defined. We found that non-selective inhibition of Ca^{2+} signaling strongly impairs many effector functions of bone marrow-derived macrophages (BMDMs) and dendritic cells (BMDCs) including phagocytosis, inflammasome activation, and priming of T cells. Surprisingly however, macrophages and DCs from mice with conditional deletion of *Stim1* and *Stim2* genes – and therefore complete inhibition of SOCE – showed no major functional defects. Their differentiation, FcR-dependent and independent phagocytosis, phagolysosome fusion, cytokine production, NLRP3 inflammasome activation and their ability to present antigens to activate T cells was preserved. Our findings demonstrate that STIM1, STIM2 and SOCE are dispensable for many critical effector functions of macrophages and DCs, which has important implications for CRAC channel inhibition as a therapeutic strategy to suppress pathogenic T cells while not interfering with myeloid cell functions required for innate immunity.

Keywords

STIM1; STIM2; SOCE; CRAC channel; calcium; macrophages; dendritic cells; DC; phagocytosis; phagolysosome; inflammasome; NLRP3; immunodeficiency

Address Correspondence to: Stefan Feske, MD Department of Pathology, Experimental Pathology Program New York University School of Medicine 550 First Avenue, Smilow 316, New York, NY 10016 Tel: (212) 263-9066, Fax: (212) 263 8211 feskes01@nyumc.org.

Conflict of interest statement: S.F. is a cofounder of Calcimedica; the other coauthors declare no conflict of interest.

Introduction

Ca^{2+} influx across the plasma membrane through Ca^{2+} release-activated Ca^{2+} (CRAC) channels is an important signaling pathway for the activation of immune cells (1). In T lymphocytes, where this pathway is best characterized, CRAC channels are activated after TCR stimulation that results in the activation of phospholipase C gamma (PLCγ), production of 1,4,5-inositol trisphosphate (IP_3), opening of IP_3 receptor channels in the membrane of the ER and release of Ca^{2+} from ER stores. Engagement of other ITAM motif-containing immunoreceptors and G protein coupled receptors on immune cells also activates PLCγ and PLCβ, respectively, and leads to IP_3 production (1). Ca^{2+} release from the ER results in a transient increase in intracellular Ca^{2+} concentrations $[Ca^{2+}]_i$ and a decrease in $[Ca^{2+}]_{ER}$. The latter causes the opening of store-operated CRAC channels in the plasma membrane (PM) via the activation of stromal interaction molecule (STIM) 1 and STIM2, which are single pass transmembrane proteins located in the ER membrane. Dissociation of Ca^{2+} from the ER luminal part of STIM proteins results in their translocation to ER-PM junctions and binding to ORAI1, the pore forming subunit of the CRAC channel (2-4). Opening of ORAI1 results in SOCE, thus called because this form of Ca^{2+} influx is regulated by the $[Ca^{2+}]_{ER}$ (5). SOCE has been demonstrated not only in T cells but also in many other types of immune cells including B cells, mast cells, macrophages, dendritic cells (DC) and neutrophils (1).

CRAC channels play an important role for immunity to infection as patients with inherited mutations in *ORAI1* and *STIM1* genes that abolish SOCE suffer from severe combined immunodeficiency (SCID)-like disease (6-8), which necessitates hematopoietic stem cell transplantation (HSCT). These patients have recurrent and chronic infections with viruses, bacteria and fungal pathogens that have been attributed to impaired T cell function because of severely impaired proliferation and cytokine production of patient T cells *in vitro*. T cell-specific deletion of *Stim1* gene expression in mice impairs immunity to *Mycobacterium tuberculosis* (9) and deletion of both *Stim1* and *Stim2* compromises antiviral immunity due to impaired $CD4^+$ and $CD8^+$ T cell responses (10). In contrast to the well documented function of CRAC channels in T cells, their role in innate immune responses is not well defined and it is unclear if defects in myeloid cells contribute to the immunodeficiency of ORAI1 and STIM1 deficient patients.

In macrophages, intracellular Ca^{2+} was shown to regulate several cell functions such as the production of TNFα and nitric oxide (NO) (11, 12). FcR-dependent and independent phagocytosis by macrophages is associated with intracellular Ca^{2+} transients (13-16). Whether phagocytosis requires cytosolic Ca^{2+} signals, however, is controversial and various studies buffering extra- and intracellular Ca^{2+} have come to different conclusions (14-17). These early studies precede the identification of ORAI1, STIM1 and STIM2 as components of the CRAC channel, thus precluding direct genetic analysis how SOCE controls phagocytosis. More recently, peritoneal macrophages from $Stim1^{-/-}$ mice were reported to have a phagocytosis defect (18). Following phagocytosis, phagosomes fuse with lysosomes in a process called phagolysosome fusion or phagosome maturation, which is required for destruction of phagocytosed pathogens. There is evidence that phagosome maturation is dependent on Ca^{2+} (19-21), although other studies demonstrated that this process is Ca^{2+}

independent or even inhibited by Ca^{2+} (22, 23). The role of SOCE in phagosome maturation, like that in phagocytosis, remains largely unknown.

In DCs, Ca^{2+} was reported to promote activation and maturation *in vitro* (24-26) and to play a role in DC responses to TLR ligands or bacteria (27-34). IP_3 or LPS stimulation of mouse bone marrow derived $CD11c^+$ DCs were shown to induce SOCE and Ca^{2+} currents resembling I_{CRAC} in T cells (25, 35). Inhibition of SOCE and Ca^{2+} currents by the non-selective inhibitor SKF-96365 decreased the LPS-induced expression of TNFα and the CCL21-dependent migration of DC while simultaneously increasing phagocytosis (35). This is consistent with the recently reported role of CRAC channels in the activation of human monocyte-derived DC *in vitro* (36). These largely inhibitor-based studies suggest that *in vitro* differentiated human and mouse DCs require SOCE, but as for macrophages, the precise role of SOCE in DC maturation and function remains poorly defined.

Ca^{2+} signals have been implicated in the regulation of NOD-like receptor family, pyrin domain containing 3 (NLRP3) inflammasome function in myeloid cells (37). The NLRP3 inflammasome is activated by various stimuli including viruses, bacterial toxins, cholesterol and monosodium urate (MSU) crystals, which result in caspase 1-dependent cleavage of pro-IL-1β and pro-IL-18 and secretion of both proinflammatory cytokines. Activation of the NLRP3 inflammasome by ATP and other stimuli was reported to require Ca^{2+} signaling as inhibition of Ca^{2+} release from the ER and blocking extracellular Ca^{2+} influx inhibited NLRP3 inflammasome function, presumably by preventing Ca^{2+} induced mitochondrial damage (38). Extracellular Ca^{2+}, which is increased at sites of infection and inflammation and acts as a danger signal, can also activate the NLRP3 inflammasome directly by binding to the calcium-sensing receptor (CASR) in the PM, which is a G protein coupled receptor that mediates the production of IP_3 and Ca^{2+} release from ER stores (39, 40). However, none of these studies directly addressed whether modulation of $[Ca^{2+}]_i$ via SOCE is involved in the regulation of NLRP3 inflammasome activation.

In this study, we investigated the specific role of SOCE in macrophage and DC function. By using macrophages and DCs from mice with conditional deletion of *Stim1* and *Stim2* genes on an inbred C57BL/6 genetic background, we show that macrophages and DC lack SOCE completely in the absence of STIM1 and STIM2. However, abolished SOCE did not result in gross abnormalities in the development of macrophages and DC *in vivo* or the differentiation of BMDMs and BMDCs *in vitro*. Despite abolished SOCE, murine macrophages showed normal FcR-dependent and independent phagocytosis and maturation of phagolysosomes. Furthermore, the production of cytokines in response to various pattern-recognition receptor (PRR) ligands and the activation of the NLRP3 and NLRC4 inflammasomes were normal in STIM1/STIM2-deficient DCs and macrophages. Lastly, the antigen-presenting function and the subsequent activation of cognate T cells remained intact in SOCE-deficient BMDCs. By contrast, many effector functions of macrophages and DCs including phagocytosis, NLRP3 inflammasome activation and antigen presentation were impaired when Ca^{2+} signaling was inhibited with non-selective Ca^{2+} channel modulators or Ca^{2+} chelating agents. Collectively, our findings demonstrate that Ca^{2+} signaling, but not SOCE via CRAC channels, is required for key effector functions of macrophages and DCs.

Materials and Methods

Mice

The generation of *Stim1*$^{fl/fl}$ and *Stim2*$^{fl/fl}$ mice was described previously (41). Mice were further crossed to *Mx1-Cre* (B6.Cg-Tg(Mx1-cre)1Cgn/J, Jackson labs [JAX] strain 003556) or *Vav1-Cre* (B6.Cg-Tg(Vav1-cre)A2Kio/J, JAX strain 008610) mice (42). OT-II^{+} mice (C57BL/6-Tg(*TcraTcrb*)425Cbn/J, JAX strain 004194) crossed to congenic CD45.1 mice (B6.SJL-*Ptprc*^{a} *Pepc*^{b}/BoyJ, JAX strain 002014) were a kind gift from Dr. Adrian Erlebacher (NYU School of Medicine). All mice were maintained on a C57BL/6 genetic background. Animals were used between 6 and 16 weeks of age. Inducible ablation of *Stim1* and *Stim2* genes in *Stim1*$^{fl/fl}$*Stim2*$^{fl/fl}$ *Mx1-cre* mice was carried out by injecting mice 3 times with 400 μg polyI:C (Sigma) every other day intraperitoneally (i.p.) as described before (43). Efficacy of *Stim1* and *Stim2* deletion was confirmed by immunoblotting and measurements of SOCE. All experiments were conducted in accordance with protocols approved by the institutional animal care and use committee (IACUC) of NYU Langone Medical Center.

Media and cell lines

Complete DMEM (supplemented with 10% heat-inactivated FCS, 1% non-essential amino acids, 1% Na-pyruvate, 1% penicillin-streptomycin, and 1% L-glutamine [all CellGro]) containing 10% CMG14-12 cell supernatant was used to differentiate BMDMs as described (44). Complete RPMI 1640 (RPMI 1640 supplemented with 10% heat-inactivated FCS, 2 mM L-glutamine, 1 mM pyruvate, 50 μM 2-mercaptoethanol, 100 U/ml penicillin, 100 μg/ml streptomycin [all CellGro]) was used to differentiate BMDCs and maintain T cell cultures. The CMG14-12 cell line was a kind gift from Dr. Ken Cadwell (NYU School of Medicine). CMG14-12 cells were grown in complete α-MEM and cell culture supernatant was harvested, sterile-filtered through a 0.45 μm filter-unit (Millipore), and tested as previously described (44).

Reagents for cell culture

BMDMs, BMDCs, and T cells were treated with EGTA (2.2 mM final concentration, Sigma), 2-Aminoethoxydiphenylborane (2-APB, 50 μM, Calbiochem), BAPTA-AM (10 μM, Invitrogen), Thapsigargin (TG, 1 μM, Calbiochem), LPS-EB (1-5 μg/ml; E. coli 0111:B4, Invivogen), curdlan (20-50 μg/ml, Invivogen), zymosan A (25-100 μg/ml, Sigma) CpG (100 nM, Invivogen), 5 or 10 MOI Bacillus Calmette-Guerin (BCG) (45), imiquimod (1 μg/ml, Invivogen), 12-*O*-tetradecanoyl-phorbol-13-acetate (PMA, 10 ng/ml, Calbiochem), ionomycin (0.2 μM, Invitrogen), ATP (3-5 mM, Invivogen), MSU crystals (150 μg/ml, Invitrogen), FlaTox (a combination of 5 μg/ml Lfn-FlaA and 10 μg/ml PA, a gift of Dr. Russell Vance, University of California, Berkeley, CA) as indicated.

Differentiation of BMDMs and BMDCs

Femur and tibia of mice were removed and bone marrow was flushed out using a 0.45 mm diameter needle and washed twice as described previously (46). For BMDMs, 5x10^{6} BM cells were cultured in 10 ml DMEM containing 10% CMG14-12 cell supernatant for 5 or 6

days, resulting in > 90% $CD11b^+F4/80^+$ cells. For BMDCs, 2.5×10^6 BM cells were cultured RPMI1640 medium supplemented with 25 ng/ml recombinant GM-CSF (Peprotech) for 8 days resulting in > 90% $CD11b^+CD11c^+$ cells.

Isolation of primary peritoneal macrophages

Mice were injected i.p. with 1 ml of 1% thioglycollate (Difco) in PBS and sacrificed 3 days later. Abdominal skin was removed (leaving the peritoneum intact), animals were injected with 10 ml sterile PBS and the peritoneum was massaged to dislodge any attached cells. Lavage fluid was extracted using a 10 ml syringe and the resulting cell suspension was washed once. Cells were re-suspended in complete DMEM and plated overnight on tissue culture plates. Non-adherent cells were removed and the remaining adherent cells were mainly $CD11b^+$ myeloid cells.

Measurements of intracellular Ca^{2+} levels

Analysis of intracellular Ca^{2+} concentrations ($[Ca^{2+}]_i$) in BMDMs and BMDCs by fluorescence microscopy was performed as previously described (47). Briefly, cells were loaded with 2 μM Fura-2-AM (Molecular Probes) for 30 min and $[Ca^{2+}]_i$ was analyzed using time-lapse imaging on an IX81 epifluorescence microscope (Olympus). For measurements of SOCE, baseline $[Ca^{2+}]_i$ was acquired in nominally Ca^{2+}-free Ringer solution (155 mM NaCl, 4.5 mM KCl, 3 mM $MgCl_2$, 10 mM D-glucose, and 5 mM Na-HEPES) followed at the indicated times by stimulation with 1 μM thapsigargin (TG) (EMD Millipore) or 0.2 μM ionomycin to deplete ER stores. To induce Ca^{2+} influx, cells were perfused with Ca^{2+}-containing Ringer solution (155 mM NaCl, 4.5 mM KCl, 2 mM $CaCl_2$, 1 mM $MgCl_2$, 10 mM D-glucose, and 5 mM Na-HEPES). For measurements of $[Ca^{2+}]_i$ in response to various PRR ligands, BMDCs were stimulated with 5 μg/ml LPS-EB (tlrl-eblps, Invivogen), 20 μg/ml curdlan (Invivogen), 100 μg/ml zymosan (Sigma), 1 μg/ml imiquimod (Invivogen), or 100 nM CpG (Invivogen) in 2 mM Ca^{2+} Ringer solution. After 420 sec, SOCE was induced with 0.2 μM ionomycin. $[Ca^{2+}]_i$ was measured as the ratio of fluorescence emission at 510 nm following excitation at 340 and 380 nm (F340/F380) and analyzed using Slidebook imaging software v4.2 (Olympus). Alternatively, F340/F380 ratios were measured in Fura-2 loaded cells with a FlexStation 3 Multi-Mode Microplate Reader (Molecular Devices) (48). BMDMs and BMDCs were plated on poly-L-lysine-coated translucent 96-well plates (BD Falcon) for 15 min, washed and incubated in 0 mM Ca^{2+} Ringer solution with or without 2.2 mM EGTA, 50 μM 2-APB, or 10 μM BAPTA-AM for 30 min before measurements of $[Ca^{2+}]_i$. Ca^{2+} influx was induced by stimulating cells with 1 μM TG as described above or by FcR cross-linking. For the latter, BMDMs were incubated with 10 μg/ml rat anti-mouse FcγIIR/FcγIIIR (CD16/CD32, clone 2.4G2, BD Pharmingen) for 30 min followed by 20 μg/ml of goat anti-rat IgG (Biolegend). Following stimulation of cells in Ca^{2+} free buffer, an equal volume of 2 mM $CaCl_2$ Ringer solution was added to cells (to obtain a final extracellular $[Ca^{2+}]$ of 1 mM). Ca^{2+} store depletion was measured as the area under the curve (AUC) after TG or ionomycin stimulation in Ca^{2+} free buffer, and the peak of Ca^{2+} influx (SOCE) was measured as the maximum F340/380 value after re-addition of extracellular Ca^{2+} minus the baseline F340/380 value at the beginning of the experiment.

Flow Cytometry

Cells were washed once in flow cytometry staining buffer (1x PBS, 0.1% BSA) before blocking with anti-FcγRII/FcγRIII (2.4G2, BD Pharmingen) for 5 min. Staining of surface molecules was performed in FACS buffer (1x PBS, 0.5% FCS) for 20 min in the dark using the following anti-mouse antibodies: anti-CD11b-PE-Cy7 or anti-CD11b-APC (clone M1/70), anti-F4/80-PerCP-Cy5.5 (BM8), anti-CD11c-eFluor450 (N418), anti-MHCII-PE or anti-MHCII-eFluor450 (I-A/I-E, M5/114.15.2), anti-CD86-APC (GL1), and anti-IFNγ-APC (XMG1.2, all eBioscience). For human PBMCs, the following antibodies were used: anti-CD3-PE-Cy7 (UCHT1), anti-CD14-AlexaFluor700 (HCD14), anti-CD19-PE-Cy7 (HIB19), anti-CD11b-BrilliantBlue 605 (M1/76), anti-HLA-DR-APC-Cy7 (L243), anti-CD303-PerCP-Cy5.5 (201A, all BioLegend). Stained cells were analyzed using a FACS LSR II flow cytometer (BD Biosciences) and FlowJo software (Tree star). For intracellular cytokine staining, OT-II$^+$ CD4$^+$ T cells were restimulated for 6 h with 20 nM PMA (Calbiochem) and 1 μM ionomycin (Invitrogen) in the presence of 3 μg/ml Brefeldin A (eBioscience). After surface staining, cells were fixed with IC Fixation Buffer and permeabilized using 1x Perm buffer (both eBioscience) according to the manufacturer's instructions.

Immunoblot analysis

Cells were harvested and resuspended in RIPA lysis buffer (50 mM Tris, 150 mM NaCl, 1% NP-40, 0.5% sodium deoxycholate, 0.1% SDS, 1 mM EDTA, 1 mM PMSF, 1 mM Na-ortho-Vanadate, and complete protease inhibitor cocktail (Sigma)) and sonicated on ice for 10 minutes. For Western blot analysis, 50-100 μg of total protein was fractionated on a 12 % SDS-PAGE and transferred onto nitrocellulose membrane. Membranes were incubated with monoclonal goat anti-mouse actin (C4, Santa Cruz Biotechnology), rabbit anti-mouse caspase-1 p10 (C-20, Santa Cruz Biotechnology), rabbit anti-mouse anti-IL-1β (D4T2D, Cell Signaling), and a custom made polyclonal rabbit antibody against the C-terminal domain of STIM1 (8). For detection, peroxidase-coupled secondary anti-goat or anti-rabbit antibodies (Sigma) and the enhanced chemiluminescence system (Thermo Scientific), or anti-goat IRDye 800CW and anti-rabbit IRDye 680LT antibodies and the Odyssey Fc Western Imaging system (Li-COR) were used.

Phagocytosis assays using beads

For FcR-independent phagocytosis, BMDMs or BMDCs were plated in 96-well plates and pre-incubated with or without 2.2 mM EGTA, 50 μM 2-APB, or 10 μM BAPTA-AM. After 30 min, yellow-green fluorescent (505/515) carboxylate-modified microspheres (Invitrogen) were added in various bead-to-cell ratios (1, 5, and 25). For FcR-dependent phagocytosis, BMDMs and BMDCs were prepared as described above and incubated with FITC-labeled IgG-coated latex beads (Cayman Chemical) at different bead-to-cell ratios (1, 5, and 25). After 2 h of culture, uptake of fluorescent beads by CD11b$^+$F4/80$^+$ BMDMs or CD11c$^+$ BMDCs, respectively, was analyzed by flow cytometry. To compare different phagocytosis experiments, ΔMFI values (MFI_{beads}-$MFI_{no\ beads}$) were calculated. For phagocytosis measurements using fluorescence microscopy, 1x10^5 BMDMs were grown on 8 well chamber slides (LabTek) over night. Cells were treated for 30 min with 10 μM BAPTA-AM or left untreated. Subsequently, BMDMs were incubated with either carboxylate-modified 1

μm yellow-green latex beads (2% solid, Invitrogen) at a 10:1 bead-to-cell ratio or FITC-labeled IgG beads (Cayman Chemical) according to the manufacturer's protocol. Cells and beads were centrifuged at 300 x g for 1 min to synchronize the initiation of phagocytosis and after 30 min washed 3 times with PBS. Cells were fixed with 4% PFA for 30 min and nuclei were stained with 2.5 μg/ml Hoechst 33342 (Molecular Probes). Images were captured using a Nikon Eclipse TiE/B automated fluorescence microscope with Photometrics HQ@ Monochrome digital camera. 60x z-stack images were acquired, and the number of latex beads or $FITC^+$ vacuoles per cell was quantified using NIS-Elements DUO software. At least 5 fields per sample with an average cell number of 15 per field were analyzed.

Phagocytosis assay using opsonized mouse RBC and *S. aureus.*

Fresh mouse red blood cells (mRBCs) were extracted from the blood of WT C57BL/6 mice using Ficoll-Plaque gradient centrifugation and washed once with PBS. 200 μl of mRBC solution were opsonized with 25 μl anti-mouse RBC antibody (34-3C, Abcam) for 1 hour and labeled with 8 μl of anti-Ter119-PE antibody. After washing twice with PBS, 2, 20, or 200 opsonized mRBCs per cell were incubated with BMDMs or peritoneal macrophages for 3 hours. Phagocytosis was analyzed by measuring $Ter119^+$ cells using flow cytometry. GFP-expressing *S. aureus* (Newman strain) was a gift of Dr. Victor Torres (NYU School of Medicine) (49). *S. aureus* was harvested during the logarithmic growth phase and incubated at 1, 10, or 50 MOI with BMDMs for 2 h. Phagocytosis was analyzed testing the uptake of GFP-expressing bacteria in $CD11b^+$ cells by flow cytometry and fluorescence microscopy using a automated Nikon Eclipse TiE/B system with Photometrics HQ@ Monochrome digital camera and NIS-Elements DUO software package.

Lysosomal trafficking assays

GFP-expressing *S. aureus* (Newman strain) were harvested during their logarithmic-growth phase and incubated with BMDMs at an MOI of 10 for 60 and 120 min. LysoTracker-Red (Invitrogen) was added to BMDMs 30 min before the end of the incubation period and extracellular *S. aureus* were lysed with Lysostaphin (Sigma). Cells were fixed with 4% PFA in PBS and confocal images were acquired with an inverted Zeiss LSM510 laser scanning confocal microscope and a 60x NA 1.45 oil-immersion objective (Zeiss). Image analysis was done using ImageJ software (NIH). The percentage of phagocytosed *S. aureus* colocalizing with LysoTracker-Red was determined by blinded counting. To study trafficking of phagocytosed mycobacteria to lysosomes, BMDMs were infected with 10 MOI of GFP-expressing Bacille Calmette-Guerin (BCG, an attenuated strain of *M. bovis*) (45) for 3 h, then washed 3 times with media and incubated another 24 h in RPMI medium at 37°C. Cells were washed once and fixed with 4% PFA in PBS for 30 min, permeabilized with 0.1% saponin in PBS for 5 min and incubated with polyclonal rabbit anti-LAMP1 antibody (Abcam). Images were captured using a Nikon Eclipse TiE/B automated fluorescent microscope with Photometrics HQ@ Monochrome digital camera. 60x z-stack images were acquired and analyzed using NIS-Elements DUO software as previously described (45).

Cytokine ELISA

1×10^6 BMDMs or BMDCs per ml were left untreated or stimulated with 1 μg/ml LPS-EB (tlrl-eblps, Invivogen), 50 μg/ml Curdlan (Invivogen), 25 μg/ml zymosan A (Sigma), 100 nM CpG (Invivogen), 5 MOI Bacillus Calmette-Guerin (*M. bovis*-BCG) (45), or 1 μg/ml Imiquimod (Invivogen) for 16 h. Cytokine concentrations in supernatants were analyzed with the Ready-Set-Go ELISA kits detecting mouse IL-1β, IL-2, IL-6, IL-10, IL-12p40, IL-12p70, IL-23p19, and TNFα (all eBioscience) according to the manufacturer's instructions and measured at 450 nm with a SpectraMax M5 ELISA reader (Molecular Devices).

NLRP3 and NLRC4 inflammasome activation

For NLRP3 inflammasome activation, BMDMs and BMDCs were plated at a density of $1x10^6$ cells per ml, primed with 10 μg/ml LPS for 4 hours (with or without 2.2 mM EGTA, 50 μM 2-APB, or 10 μM BAPTA-AM) and stimulated for 30 min with 3 mM ATP (Invivogen). Alternatively, the NLRP3 inflammasome was activated by stimulation with 150 μg/ml MSU crystals (Invitrogen) for 4 h. For NLRC4 inflammasome activation, cells were incubated for 15 or 30 min with a combination of 5 μg/ml Legionella pneumophila flagellin (FlaA) fused to the amino-terminal domain of Bacillus anthracis lethal factor (LFn) and 10 μg/ml recombinant anthrax protective antigen (PA), referred to as FlaTox (gift of Dr. Russell Vance, University of California, Berkeley). Following stimulation, cell culture supernatants were harvested and analyzed for IL-1β secretion by ELISA and cells were lysed and analyzed for pro-caspase 1 cleavage by WB.

Antigen presentation and T cell activation assay

BMDCs were maturated into antigen-presenting cells (APC) with 0.1 μg/ml LPS with or without 10 μM BAPTA-AM for 30 min. After washing, BMDMs or BMDCs were incubated overnight with 0.5 mg/ml ovalbumin (OVA) protein (Sigma). OVA-specific $CD4^+$ T cells were isolated from the spleen and LNs of OT-II mice using the EasyStep Mouse $CD4^+$ T Cell Enrichment Kit (StemCell Technologies). $CD4^+$ T cells were labeled with 2.5 μM CellTrace CFSE (Invitrogen) for 5 min and washed twice. Unbound OVA was removed from APC cultures before co-culturing with CFSE-labeled OT-II $CD4^+$ T cells in 5:1 and 1:1 APC to T cell ratios. After 72 hours, proliferation (i.e. CFSE-dilution) was analyzed by flow cytometry. As a negative control, OT-II T cells were incubated with BMDCs without OVA protein and, as a positive control, OT-II T cells were stimulated polyclonally using anti-CD3 and anti-CD28 mAbs (145-2C11 and 37.51, both eBioscience). For the detection of intracellular IFNγ OT-II T $CD4^+$ cells were restimulated with 20 nM PMA (Calbiochem) and 1 μM ionomycin (Invitrogen) in presence of 3 μg/ml Brefeldin A (eBioscience) for 6 h and analyzed by flow cytometry.

Patient samples

Frozen PBMCs from a healthy donor and a SOCE-deficient patient homozygous for the $ORAI1^{R91W}$ mutation (2) were thawed and 5×10^5 cells were stained for cell surface markers to determine monocyte and DC populations and analyzed by flow cytometry.

Informed consent for the studies was obtained from the patient's family in accordance with the Declaration of Helsinki and IRB approval of NYU School of Medicine.

Statistical analysis

Experimental data were analyzed with Prism software (GraphPad) and statistical significance was calculated by two-tailed paired or unpaired Student's t test. Differences with p values of < 0.05 were considered to be statistically significant: *, $p < 0.05$; **, $p < 0.005$, and ***, $p < 0.001$, respectively.

Results

STIM1 and STIM2 are not required for the differentiation of macrophages and DCs

STIM1 was shown to mediate SOCE in macrophages (18), DCs (36) and neutrophils (50). It therefore seemed likely that innate immune responses require SOCE and that abolished SOCE in patients with loss-of-function or null mutations in *ORAI1* and *STIM1* genes may contribute to their immunodeficiency. We and others had previously described that ORAI1 and STIM1 deficient patients have normal numbers of monocytes, neutrophils, basophils and eosinophils in their peripheral blood, suggesting that SOCE mediated by CRAC channels is not required for the development of myeloid cells (7, 8, 51). Accordingly, we found that the frequencies of $CD14^+$ $CD303^-$ monocytes, $CD14^-$ $CD303^-$ conventional DCs (cDCs), and $CD14^-$ $CD303^+$ plasmacytoid DCs (pDCs) were comparable in the peripheral blood of a five months old patient with a homozygous R91W loss-of-function mutation in ORAI1 (referred to as $ORAI1^{R91W}$) (2) and a healthy donor control (**Figure S1**).

Since patients with genetic defects in *ORAI1* and *STIM1* genes are very rare and surviving patients have leukocyte chimerism after HSCT, it is difficult to study the role of SOCE in innate immunity in human patients. Various studies have used human or mouse myeloid cell lines or primary cells and investigated Ca^{2+} signaling either by chelating extra- or intracellular Ca^{2+} (with EGTA or BAPTA) or by using non-selective Ca^{2+} channels inhibitors (36, 52-54). Since these approaches do not specifically inhibit CRAC channels and SOCE, we decided to use mice with conditional deletion of *Stim1* and *Stim2* genes in hematopoietic cells (41). These mice were generated on a defined inbred C57BL/6 genetic background to avoid confounding effects by genes not related to CRAC channel function. First, we ablated STIM protein expression in $Stim1^{fl/fl}$ *Mx1-Cre* or $Stim1^{fl/fl}Stim2^{fl/fl}$ *Mx1-Cre* mice by polyI:C injection (41, 43). To rule out any potential immunological artifacts arising from the transient type I interferon response induced by polyI:C, we also generated $Stim1^{fl/fl}Stim2^{fl/fl}$ *Vav-Cre* mice, in which *Stim1* and *Stim2* are conditionally deleted in all hematopoietic cells without any further treatment (55). Hematopoietic precursor cells from both strains of mice were then differentiated into BMDMs and dendritic cells BMDCs *in vitro*.

The efficiency of STIM1 and STIM2 protein deletion in BMDMs from WT, $Stim1^{fl/fl}$ *Mx1-Cre* and $Stim1^{fl/fl}Stim2^{fl/fl}$ *Mx1-Cre* was analyzed by Ca^{2+} imaging (**Figure 1a**). Deletion of STIM1 alone or both STIM1 and STIM2 strongly impaired SOCE in BMDMs from polyI:C injected $Stim1^{fl/fl}$ *Mx1-Cre* mice andabolished in BMDMs from polyI:C injected

Stim1$^{fl/fl}$*Stim2*$^{fl/fl}$ *Mx1-Cre* mice (**Figure 1a,** and data not shown) when SOCE was induced with thapsigargin (TG), an inhibitor of the sarco/endoplasmic reticulum ATPase (SERCA) pump, or ionomycin, which leaks Ca^{2+} from ER stores. By contrast, deletion of STIM1 alone or both STIM1 and STIM2 had no significant effect on Ca^{2+} store depletion. The absence of STIM1 protein in BMDMs from *Stim1*$^{fl/fl}$ *Mx1-Cre* and *Stim1*$^{fl/fl}$*Stim2*$^{fl/fl}$ *Mx1-Cre* mice was confirmed by Western blotting (**Figure 1b**). Despite the severe defect in SOCE, the numbers and immunological phenotype of BMDMs from *Stim1*$^{fl/fl}$ *Mx1-Cre* and *Stim1*$^{fl/fl}$*Stim2*$^{fl/fl}$ *Mx1-Cre* mice were comparable to WT controls (**Figure 1c**) suggesting that SOCE is not required for the differentiation of BMDMs *in vitro.* Similar results were obtained using BMDMs from *Stim1*$^{fl/fl}$*Stim2*$^{fl/fl}$ *Vav-Cre* mice, which lacked SOCE (**Figure 1d)** but like WT BMDMs were > 99% F4/80^{+} Cd11b^{+} (**Figure 1e**). We next tested the effects of STIM1 and STIM2 deletion in BMDCs generated from *Stim1*$^{fl/fl}$*Stim2*$^{fl/fl}$ *Vav-Cre* BM cells (**Figure 1f-1h**). STIM1/STIM2-deficient BMDCs showed unaltered Ca^{2+} store release compared to WT control cells, whereas SOCE was completely absent in response to TG (**Figure 1f**) or ionomycin (data not shown) stimulation. CRAC channels and STIM1 or STIM2 were suggested to play a role in the differentiation and maturation of DCs (25, 36, 56). However, we observed normal expression of CD11c, CD86 and MHC class II on immature BMDCs generated from *Stim1*$^{fl/fl}$*Stim2*$^{fl/fl}$ *Vav-Cre* mice compared to WT controls (**Figure 1g,h**). Taken together, STIM1 and STIM2 are essential for SOCE but not the differentiation and maturation of BMDMs and BMDCs *in vitro*. We were therefore able to use BMDMs and BMDCs derived from *Stim1*$^{fl/fl}$*Stim2*$^{fl/fl}$ *Vav-Cre* and *Stim1*$^{fl/fl}$*Stim2*$^{fl/fl}$ *Mx1-Cre* mice to investigate the role of SOCE and CRAC channels in DC and macrophage function.

Ca^{2+} signaling but not SOCE is required for phagocytosis in macrophages and DCs

Ca^{2+} signals were shown in several studies to be required for macrophage phagocytosis (13-16), but the source of Ca^{2+} and the channels mediating these Ca^{2+} signals remained unclear. Earlier studies used mostly Ca^{2+} chelators to buffer extracellular and cytosolic Ca^{2+} or non-selective ion channel inhibitors (15, 16). To investigate the specific contribution of SOCE to FcR-dependent and independent phagocytosis, we analyzed BMDMs (**Figure 2** and **Figure S2**) and BMDCs (**Figure S3**) from *Stim1*$^{fl/fl}$*Stim2*$^{fl/fl}$ *Mx1-Cre* and *Stim1*$^{fl/fl}$*Stim2*$^{fl/fl}$ *Vav-Cre* mice. For comparison, we investigated the effects of extracellular and cytosolic Ca^{2+} chelation with EGTA and BAPTA-AM, respectively, and those of inhibiting Ca^{2+} influx and ER store release with the widely used but non-selective ion channel modulator 2-APB, which has complex effects on CRAC channels, TRP channels and the IP_3Rs (57-60).

Deletion of STIM1 and STIM2 in BMDMs and BMDCs completely inhibited SOCE after TG stimulation compared to WT control cells (**Figure 2a-c**; **S3a-c**). Chelation of extracellular Ca^{2+} with EGTA to prevent Ca^{2+} influx (**Figure 2a**; **S3a**), chelation of cytosolic Ca^{2+} with BAPTA-AM (**Figure 2b**; **S3b**) and treatment with 2-APB (**Figure 2c**; **S3c**) reduced the TG-induced Ca^{2+} influx in WT cells to a similar degree as deletion of *Stim1* and *Stim2* genes. No additional reduction of Ca^{2+} influx was observed in STIM1/STIM2-deficient cells after treatment with EGTA, BAPTA-AM or 2-APB compared to

control cells. These findings indicate that TG-induced SOCE in BMDMs and BMDCs is completely dependent on STIM1 and STIM2.

By contrast, *Stim1* and *Stim2* gene deletion had no effect on the release of Ca^{2+} from ER stores. The integrated Ca^{2+} signal following TG or ionomycin stimulation in Ca^{2+} free extracellular buffer was comparable in STIM1/STIM2-deficient and WT control BMDMs (**Figure 2a-c** and data not shown) and BMDCs (**Figure S3a-c** and data not shown), indicating that the filling of ER Ca^{2+} stores is intact in the absence of STIM1 and STIM2. By contrast, the $[Ca^{2+}]_i$ rise following TG-induced ER store depletion was attenuated in cells treated with 2-APB, EGTA and especially BAPTA (**Figure 2a-c, S3a-c**), indicating that these agents perturb the filling state of ER Ca^{2+} stores by interfering with other Ca^{2+} signaling pathways besides SOCE. STIM1/STIM2-deficient mice and the non-selective inhibitors of Ca^{2+} signaling allowed us to distinguish between the specific contributions of SOCE (absent in STIM1/STIM2-deficient cells), Ca^{2+} influx via SOCE plus other plasma membrane Ca^{2+} channels (inhibited by 2-APB and EGTA), and Ca^{2+} release from intracellular stores plus Ca^{2+} influx (neutralized by BAPTA) to BMDM and BMDC function.

To evaluate the role of SOCE and Ca^{2+} signals in phagocytosis, we first analyzed the FcR-independent uptake of fluorescent latex beads by BMDMs (**Figure 2d, S2a**) and BMDCs (**Figure S3d**). *Stim1*$^{fl/fl}$*Stim2*$^{fl/fl}$ *Vav-Cre* and WT control BMDMs were left untreated or pre-treated with EGTA, BAPTAAM or 2-APB and incubated with latex beads at different bead-to-cell ratios (1:1, 5:1 and 25:1). Flow cytometric analysis did not show a difference in phagocytosis by BMDMs from *Stim1*$^{fl/fl}$ *Mx1-Cre*, *Stim1*$^{fl/fl}$*Stim2*$^{fl/fl}$ *Mx1-Cre* (**Figure S2a**) or *Stim1*$^{fl/fl}$*Stim2*$^{fl/fl}$ *Vav-Cre* mice (**Figure 2d**) compared to WT controls. Likewise, inhibition of Ca^{2+} influx with 2-APB or EGTA did not substantially impair phagocytosis of STIM1/STIM2-deficient or WT macrophages (**Figure 2d**). By contrast, chelation of intracellular Ca^{2+} with BAPTA significantly reduced phagocytosis by BMDMs (**Figure 2d**). Similar results were obtained using fluorescence microscopy to analyze phagocytosis (**Figure 3a,b**). Furthermore, we found that phagocytosis of latex beads in BMDCs is independent of STIM1 and STIM2 (**Figure S3d**). We next tested the FcR-independent phagocytosis of bacteria by incubating BMDMs with live GFP-expressing *Staphylococcus aureus* (*S. aureus*). Bacterial phagocytosis was unaltered in BMDMs from *Stim1*$^{fl/fl}$ *Mx1-Cre* and *Stim1*$^{fl/fl}$*Stim2*$^{fl/fl}$ *Mx1-Cre* mice (**Figure S2b**). Together these data show that FcR-independent phagocytosis is regulated by cytosolic Ca^{2+} levels but independent of SOCE mediated by STIM1 and STIM2.

FcR crosslinking results in STIM1-dependent SOCE that was shown to be required for FcR-dependent phagocytosis (18). We confirmed that crosslinking of FcγRII/III (CD16/32) results in rapid SOCE in WT control BMDMs, which was almost completely abolished in BMDMs from *Stim1*$^{fl/fl}$*Stim2*$^{fl/fl}$ *Vav-Cre* BMDMs (**Figure S2c**). To evaluate if STIM1 and STIM2 are required for FcR-mediated phagocytosis, we incubated BMDMs with fluorescent IgG-coated beads (**Figure 2e, S2d**) and antibody-opsonized mouse RBCs (**Figure S2e**). Surprisingly, the phagocytosis of IgG-coated beads by BMDMs from *Stim1*$^{fl/fl}$ *Mx1-Cre* mice, *Stim1*$^{fl/fl}$*Stim2*$^{fl/fl}$ *Mx1-Cre* mice (**Figure S2d**) and *Stim1*$^{fl/fl}$*Stim2*$^{fl/fl}$ *Vav-Cre* mice (**Figure 2e**) was comparable to WT controls. Normal phagocytosis of antibody-opsonized

mRBCs was also observed in BMDMs (**Figure S2e**) and, importantly, in primary peritoneal macrophages from polyI:C-treated *Stim1*$^{fl/fl}$ *Mx1-Cre* or *Stim1*$^{fl/fl}$*Stim2*$^{fl/fl}$ *Mx1-Cre* mice compared to WT controls (**Figure S2f**). Together these findings demonstrate that STIM1 and STIM2 are not required for FcR-dependent phagocytosis by *in vitro* differentiated and peritoneal macrophages. Treatment of BMDMs with 2-APB had no effect on the phagocytosis of IgG-coated beads, whereas chelation of extracellular Ca^{2+} with EGTA partially, and chelation of cytosolic Ca^{2+} with BAPTA completely inhibited phagocytosis (**Figure 2e**). Similar results were obtained in BMDCs (**Figure S3e**). The effect of BAPTA on the phagocytosis of IgG-coated beads was more pronounced compared to non-coated beads when analyzed either by flow cytometry (**Figure 2d,e**) or fluorescence microscopy (**Figure 3c,d**), suggesting that cytosolic Ca^{2+} signaling may be more critical for FcR-dependent phagocytosis. Taken together, our results demonstrate that whereas intracellular Ca^{2+} signals are required for FcR-dependent and -independent phagocytosis by macrophages and DCs, SOCE mediated by STIM1 and STIM2 is dispensable for this process.

Lysosomal trafficking is independent of STIM1 and STIM2

Following phagocytosis, endosomes fuse with Golgi apparatus-derived lysosomes that contain hydrolytic enzymes. This process of phagolysosome fusion is required for the degradation of phagocytosed pathogens and the production of pathogen-derived peptides presented on MHC class II molecules. The involvement of Ca^{2+} signals in lysosomal trafficking and phagolysosome fusion is debated (19-23) and the specific role of SOCE in this process has not been investigated. We therefore analyzed intracellular trafficking and colocalization of live GFP-expressing *S. aureus* with lysosomes in BMDMs from WT and *Stim1*$^{fl/fl}$*Stim2*$^{fl/fl}$ *Mx1-Cre* mice (**Figure 4a,b**). The phagocytosis of *S. aureus* was not impaired in STIM1/STIM2-deficient BMDMs as the number of GFP^+ bacteria per cell was comparable to WT control cells **(Figure 4c**), consistent with results obtained by flow cytometry (**Figure S2b**). We did not detect differences in the distribution pattern (**Figure 4a**) or extent (**Figure 4b**) of co-localization between *S. aureus* and LysoTracker-positive vesicles in WT and *Stim1*$^{fl/fl}$*Stim2*$^{fl/fl}$ *Mx1-Cre* BMDMs.

Using a second pathogen, we incubated live GFP-expressing Bacillus Calmette-Guerin (BCG-GFP), an attenuated vaccine strain of *Mycobacterium bovis*, for 3 h with BMDMs from WT, *Stim1*$^{fl/fl}$ *Mx1-Cre* and *Stim1*$^{fl/fl}$*Stim2*$^{fl/fl}$ *Mx1-Cre* mice (**Figure 4d,e**). After removal of extracellular bacteria, BMDMs were cultivated for another 24 h before co-localization of GFP and lysosomal-associated membrane protein (LAMP-1), a widely-used marker for lysosomes, was evaluated by confocal microscopy (**Figure 4d,e**) (45). Quantification of the LAMP-1 signal surrounding the internalized GFP-tagged BCG showed a similar extent of colocalization in BMDMs from *Stim1*$^{fl/fl}$ *Mx1-Cre* and *Stim1*$^{fl/fl}$*Stim2*$^{fl/fl}$ *Mx1-Cre* mice compared to WT controls (**Figure 4e**), indicating that intracellular trafficking of mycobacteria into LAMP-1 positive organelles was not altered. Taken together, our findings show that SOCE mediated by STIM1 and STIM2 is dispensable for phagolysosome fusion in macrophages.

Cytokine production by BMDMs and BMDCs does not require SOCE

With degradation of internalized pathogens, so called 'danger signals' or pathogen-associated molecular pattern (PAMPs) are released and trigger maturation and activation of myeloid cells. Various pattern-recognition receptors (PRRs) were reported to induce Ca^{2+} signals (27-29, 31, 33, 61-63) and the involvement of SOCE therein has been discussed (29, 31, 36). Ca^{2+} signals are well known to mediate the activation of transcription factors such as the nuclear factor of activated T cells (NFAT) and nuclear factor κB (NF-κB) and thereby the expression of cytokines (64). To evaluate the role of SOCE in regulating cytokine production in myeloid cells, we stimulated BMDMs and BMDCs from *Stim1*$^{fl/fl}$*Stim2*$^{fl/fl}$ *Vav-Cre* and WT mice with various synthetic or natural PRR ligands that have been shown to induce Ca^{2+} signals including LPS (detected by CD14/TLR4) (29, 65, 66), CpG (TLR9) (27, 28), imiquimod (TLR7) (62, 63), curdlan and zymosan (both recognized by Dectin-1 and/or TLR2) (32-34, 67), and live Bacillus Calmette-Guerin (BCG, presumably triggering several PRRs) (**Figure 5**). Zymosan and curdlan are likely to induce SOCE as their binding to Dectin-1 activates Syk and PLCγ resulting in IP_3 production and ER store release (34, 67). For other ligands such as LPS, CpG and imiquimod the source of Ca^{2+} is not known. Surprisingly, BMDMs and BMDCs from *Stim1*$^{fl/fl}$*Stim2*$^{fl/fl}$ *Vav-Cre* produced similar amounts of TNFα, IL-6, IL-10, IL-12p70, IL-23p19, IL-2, and IL-12/23p40 as WT cells when stimulated with LPS, CpG, zymosan, curdlan, BCG or imiquimod for 16 h (**Figure 5a,b**) indicating that STIM1 and STIM2, and thereby SOCE, are dispensable for PRR-induced cytokine production in myeloid cells. To investigate if PRR ligands induce Ca^{2+} signals and whether these depend on STIM1 and STIM2, we measured Ca^{2+} influx in WT and STIM1/STIM2-deficient BMDCs in response to LPS, CpG, zymosan, curdlan or imiquimod stimulation (**Fig. S4**). In WT BMDMs, we observed small transient rises in $[Ca^{2+}]_i$ in response to LPS and zymosan, whereas stimulation with curdlan, imiquimod or CpG failed to result in Ca^{2+} increases. Even after LPS and zymosan stimulation, only few cells within the entire cell population exhibited marked Ca^{2+} influx and the magnitude of Ca^{2+} influx was small compared to that induced by ionomycin as a control to mediate SOCE (**Figure S4a,c**). The Ca^{2+} signals following LPS and zymosan stimulation were largely absent in STIM1/STIM2-deficient BMDCs compared to WT cells (although differences were not statistically significant), suggesting that they may be mediated by SOCE (**Figure S4b,c**). Taken together, PRR ligands such as LPS and Zymosan induce weak Ca^{2+} influx that may be partially mediated by SOCE, but these signals are dispensable for PRR-induced cytokine production in BMDMs and BMDCs.

Cytosolic Ca^{2+} but not SOCE is required for NLRP3 and NLRC4 inflammasome activation

Another mechanism by which innate immune cells produce pyrogenic cytokines is through activation of inflammasomes. Several studies have linked Ca^{2+} signaling to the activation of NLRP3 and NLRC4 inflammasomes (38-40, 68, 69). Ca^{2+} release from the ER (38-40, 53) and binding of extracellular Ca^{2+} to the CASR (38, 40) were described to modulate NLRP3 activation. However, most of these studies relied on the use of Ca^{2+} chelators or non-selective ion channel inhibitors (53, 54, 68, 69) and the specific role of SOCE in inflammasome activation has not been investigated. To elucidate if Ca^{2+} signals and SOCE are required for NLRP3 activation, we first stimulated WT BMDMs with LPS for 4h

followed by stimulation with ATP for 30 min. WT BMDMs secreted readily detectable amounts of IL-1β, which were significantly reduced by treatment of cells with 2-APB and abolished by chelation of intracellular Ca^{2+} with BAPTA (**Figure 6a**), indicating that Ca^{2+} signals are indeed required for NLRP3 function. Chelating extracellular Ca^{2+} with EGTA, by contrast, had no effect on IL-1β production.

ATP was shown to activate the NLRP3 inflammasome by opening P2X7 receptor channels that, besides causing K^+ efflux, mediate Ca^{2+} influx into cells (70). In addition to P2X7 receptors, ATP binds to G protein coupled P2Y receptors that induce SOCE via activation of PLCβ and production of IP_3. We therefore measured Ca^{2+} influx in STIM1/STIM2-deficient BMDMs and BMDCs following stimulation with 5 mM ATP (**Figure 6b,g**). We observed moderately reduced Ca^{2+} influx in STIM1/STIM2-deficient cells compared to WT cells which is likely due to impaired P2Y receptor-induced SOCE. To analyze if SOCE is required for NLRP3 activation, we next tested BMDMs from WT and *Stim1*$^{fl/fl}$*Stim2*$^{fl/fl}$ *Vav-Cre* mice. STIM1/STIM2-deficient BMDMs produced copious amounts of IL-1β comparable to WT cells (**Figure 6c**) despite reduced ATP-induced Ca^{2+} influx. Consistent with normal IL-1β secretion, BMDMs from *Stim1*$^{fl/fl}$*Mx1-Cre* and *Stim1*$^{fl/fl}$*Stim2*$^{fl/fl}$ *Mx1-Cre* mice showed normal cleavage of pro-caspase-1 into (active) caspase-1 (p10) after LPS and ATP stimulation that was comparable to WT BMDMs (**Figure 6d**). To distinguish between a potential role of SOCE in the priming and activation of the NLRP3 inflammasome, we analyzed the intracellular pro-IL-1β levels during the priming phase with LPS and the cleavage-induced decrease of intracellular pro-IL-1β upon ATP stimulation (**Figure 6e**). We found comparable expression levels of pro-IL-1β in BMDMs from *Stim1*$^{fl/fl}$*Stim2*$^{fl/fl}$ *Vav-Cre* and WT mice over the entire LPS stimulation period of 16 h (**Figure 6e**, left panel) and a comparable decrease of intracellular pro-IL-1β in WT and STIM1/STIM2 deficient BMDMs after ATP treatment (**Figure 6e**, right panel).

IL-1β production was also normal after treatment of STIM1/STIM2-deficient BMDMs with monosodium urate (MSU) crystals, another ‘danger signal‘ that activates the NLRP3 inflammasome (**Figure 6c**). In addition to NLRP3, we also investigated the role of SOCE in the function of the NLRC4 inflammasome, which is activated by bacterial flagellin and whose activation had been linked to Ca^{2+} influx (52). Stimulation of LPS-primed BMDMs with the bacterial toxin FlaTox that selectively activates the NLRC4 inflammasome (52) resulted in comparable IL-1β secretion in WT and STIM1/STIM2-deficient macrophages (**Figure 6f**). Normal NLRP3 and NLRC4 inflammasome activation by ATP, MSU crystals and FlaTox, respectively, was also observed in BMDCs from *Stim1*$^{fl/fl}$*Stim2*$^{fl/fl}$ *Vav-Cre* mice (**Figure 6g-i**). Taken together, our findings show that Ca^{2+} influx and SOCE are not required for NLRP3 and NLRC4 function.

Antigen presentation and stimulation of T cells by BMDCs is independent of STIM1 and STIM2

Many of the macrophage and DC functions we investigated above are required to initiate an adaptive immune response by T cells. This includes presentation of peptides from phagocytosed pathogens on MHC class II complexes, expression of co-stimulatory molecules and cytokine production. Ca^{2+} signals have been implicated in all of these steps

(24-26, 36). Ca^{2+} influx via CRAC channels was suggested to regulate expression of MHC class II and the co-stimulatory molecules CD80 and CD86 on APCs (25, 71), and siRNA mediated suppression of STIM1 and ORAI1 was shown to impair the maturation of human DCs (36).

We therefore investigated if SOCE is required for the antigen-presenting function of DC during an adaptive immune response. A comparable small fraction of BMDCs from *Stim1*$^{fl/fl}$*Stim2*$^{fl/fl}$ *Vav-Cre* and WT mice spontaneously showed a mature MHCII^{hi} CD86^{hi} phenotype without stimulation (**Figure 1g, 7a,b**). Stimulation of immature BMDCs derived from WT and *Stim1*$^{fl/fl}$*Stim2*$^{fl/fl}$ *Vav-Cre* mice with different PRR ligands including LPS, curdlan, imiquimod, CpG or zymosan dramatically increased the percentage of MHCII^{hi} CD86^{hi} mature DCs. However no significant differences between WT and *Stim1*$^{fl/fl}$*Stim2*$^{fl/fl}$ *Vav-Cre* BMDCs were observed (**Figure 7b**). Next, we analyzed the effects of STIM1/STIM2 deletion in BMDCs on T cell activation. BMDCs from WT and *Stim1*$^{fl/fl}$*Stim2*$^{fl/fl}$ *Vav-Cre* mice were incubated with ovalbumin (OVA) protein overnight, matured by stimulation with LPS and co-cultured with naïve CFSE-labeled OT-II CD4^{+} T cells, which express a transgenic TCR specific for chicken ovalbumin 323-339.The proliferation of OT-II T cells co-cultured for 72 hours with ovalbumin-loaded *Stim1*$^{fl/fl}$*Stim2*$^{fl/fl}$ *Vav-Cre* BMDCs was comparable to OT-II T cells incubated with WT BMDCs (**Figure 7c,d**).

Because we had found that several BMDM and BMDC functions were impaired when cytosolic Ca^{2+} was chelated with BAPTA, we tested its effects on antigen presentation of DCs by treating WT and STIM1/STIM2-deficient BMDCs with BAPTA for 30 minutes before co-culture with cognate T cells **(Figure 7c,d**). BAPTA significantly reduced T cell proliferation irrespective of whether T cells were co-incubated with WT or STIM1/STIM2-deficient BMDCs. These findings are consistent with the strongly impaired phagocytosis of BAPTA-treated BMDCs (**Figure S3d,e**), which limits the MHC class II-restricted presentation of cognate ovalbumin-derived peptides to OT-II T cells. In addition to proliferation, we analyzed IFNγ production by OT-II T cells that were co-incubated with WT and STIM1/STIM2 deficient BMDCs for 72h and re-stimulated with PMA and ionomycin for 6h but did not observe a significant difference in the frequency of IFNγ-positive T cells incubated with WT or STIM1/STIM2-deficient BMDCs (**Figure 7e**). By contrast, chelation of cytosolic Ca^{2+} in BMDCs with BAPTA for 30 minutes before co-culture with OT-II T cells almost completely abolished IFNγ production. Taken together, our data demonstrate that the antigen presenting function of DC and their ability to stimulate T cells depends on cytosolic Ca^{2+} signals but is independent of SOCE mediated by STIM1 and STIM2.

Discussion

SOCE via CRAC channels is a conserved Ca^{2+} influx pathway in most, if not all, immune cells, but the contribution of SOCE to the function of myeloid immune cells and innate immune responses is largely unknown. Patients lacking SOCE due to mutations in *ORAI1* or *STIM1* genes are severely immunodeficient and suffer from recurrent, often life-threatening infections with viral, bacterial, mycobacterial and fungal pathogens (6). While many infections can be attributed to impaired T cell-mediated adaptive immunity (6, 9, 10, 72), the

patients' frequent bacterial and mycobacterial (BCG) infections could be compounded by defective SOCE in innate immune cells resulting in an impaired function of neutrophils, macrophages and DCs. Consistent with the essential role of STIM1 and STIM2 in SOCE in T cells (41) and B cells (73), we found that conditional deletion of *Stim1* and *Stim2* genes in hematopoietic cells of mice completely abolishes SOCE in macrophages and DCs. Surprisingly, however, the complete lack of SOCE in these cells did not have a significant effect on any of their innate immune functions including FcR-dependent and independent phagocytosis, phagolysosome fusion, cytokine production in response to various PRR ligands, activation of NLRP3 and NLRC4 inflammasomes and antigen presentation to T cells. By contrast, abolishing Ca^{2+} signaling by chelation of $[Ca^{2+}]_i$ with BAPTA or the non-selective modulation of Ca^{2+} and other ion channels with 2-APB perturbed many macrophage and DC functions (**Figure 8**). We therefore conclude that intracellular Ca^{2+} signals are essential for the function of macrophages and DCs, whereas SOCE mediated by STIM1/STIM2 is dispensable. The apparently redundant role of SOCE in macrophages and DCs is in contrast to some earlier reports that had shown a role of STIM1 in phagocytosis by macrophages and in human DC maturation and cytokine production (18, 36). We here discuss potential causes for these discrepancies.

Our data demonstrate that FcR-dependent and independent phagocytosis of latex beads, opsonized cells (RBCs), living bacteria (*S. aureus*) and mycobacteria (BCG) by murine macrophages and DCs does not require STIM1 and STIM2 despite abolished SOCE. Normal phagocytosis is not limited to *in vitro* cultured BMDMs because primary peritoneal macrophages isolated from STIM1/STIM2 deficient mice were able to phagocytose opsonized RBCs normally. Removal of extracellular Ca^{2+} with EGTA partially impaired FcγR-dependent phagocytosis and suppression of all intracellular Ca^{2+} signaling with BAPTA significantly reduced phagocytosis. Our data are consistent with observations that phagocytosis of IgG-coated beads and RBCs in the absence of extracellular Ca^{2+} or chelation of $[Ca^{2+}]_i$ as was impaired in mouse peritoneal macrophages and the macrophage cell line J774 (15, 16). This dependence of FcγR mediated phagocytosis on intracellular Ca^{2+} was, however, not observed in other studies in which removal of extracellular Ca^{2+} or buffering intracellular Ca^{2+} had no effect on phagocytosis of IgG-coated particles or RBCs (13, 14); the cause of these differences is not known. Importantly, our data demonstrate that phagocytosis is independent of SOCE mediated by STIM1 and STIM2. This is in contrast to a report showing strongly reduced phagocytosis of IgG2a and IgG2b opsonized RBCs in $F4/80^+$ peritoneal macrophages from *Stim1*$^{-/-}$ mice (18). STIM1-deficient macrophages had impaired Ca^{2+} influx after crosslinking of FcγII/IIIa receptors. *In vivo*, *Stim1*$^{-/-}$ mice injected with antibodies against RBCs and platelets were protected from autoimmune hemolytic anemia (AIHA) and thrombocytopenia, respectively, which in the case of AIHA was attributed to impaired phagocytosis of RBCs by Kupffer cells in the liver (18). It is noteworthy to mention that patients with loss-of-function mutations in the *STIM1* gene that abolish SOCE develop anti-RBC and anti-platelet autoantibodies and, in contrast to *Stim1*$^{-/-}$ mice, suffer from AIHA and thrombocytopenia. This suggests that removal of autoantibody-bound RBCs and platelets by the mononuclear phagocyte system occurs normally in SOCE-deficient patients (8, 72).

The cause of the discrepant results obtained in *Stim1*$^{-/-}$ mice (18) compared to *Stim1*$^{fl/fl}$*Stim2*$^{fl/fl}$ *Vav-Cre* or *Stim1*$^{fl/fl}$*Stim2*$^{fl/fl}$ *Mx1-Cre* mice used in this study and the *STIM1* mutated human patients (8) is not understood. Different degrees of SOCE deficiency in cells from *Stim1*$^{-/-}$ (18) and *Stim1*$^{fl/fl}$*Stim2*$^{fl/fl}$ *Vav-Cre* or *Stim1*$^{fl/fl}$*Stim2*$^{fl/fl}$ *Mx1-Cre* mice are unlikely to account for the divergent effects on phagocytosis since SOCE appears to be more profoundly impaired in STIM1/STIM2 double-deficient than *Stim1*$^{-/-}$ macrophages. It is possible that peritoneal macrophages are more dependent on SOCE than BMDMs; however, peritoneal macrophages from *Stim1*$^{fl/fl}$ *Mx1-Cre* and *Stim1*$^{fl/fl}$*Stim2*$^{fl/fl}$ *Mx1-Cre* mice showed a normal ability to phagocytose antibody-opsonized RBCs. A potential explanation for the impaired phagocytosis by macrophages from *Stim1*$^{-/-}$ (18) but not *Stim1*$^{fl/fl}$*Stim2*$^{fl/fl}$ *Vav-Cre* or *Stim1*$^{fl/fl}$*Stim2*$^{fl/fl}$ *Mx1-Cre* mice may be that *Stim1*$^{-/-}$ mice are on a different genetic background compared to the *Stim1*$^{fl/fl}$*Stim2*$^{fl/fl}$ *Vav-Cre* and *Stim1*$^{fl/fl}$*Stim2*$^{fl/fl}$ *Mx1-Cre* mice, which are on a pure C57BL/6 background. It is possible that phagocytosis by *Stim1*$^{-/-}$ macrophages (18) is confounded by polymorphisms in modifier genes that co-regulate phagocytosis. A striking example of such a modifier effect on phagocytosis was shown by Nuvolone *et al.* who demonstrated that the phagocytosis defect in *Prnp*$^{-/-}$ mice reported in one study was not due to the lack of prion protein PrP^{c} but was linked to a genetic polymorphism in the locus for signal regulatory protein α (*Sirpa*) (74). A similar effect unrelated to STIM1 and SOCE might account for the phagocytosis defect in macrophages from *Stim1*$^{-/-}$ mice (18). Since the *Stim1*$^{-/-}$ mice used for these studies were BM radiation chimeras, it is also possible that phagocytosis is affected by the irradiation-associated inflammation.

One of the best characterized functions of SOCE in lymphocytes is the regulation of cytokine production through Ca^{2+} dependent transcription factors such as NFAT, ERK1 and NF-kB (64, 75). In T cells, the expression of IL-2, IL-4, IFNγ, TNFα, IL-17 and many other cytokines is regulated by SOCE and deletion of STIM1 or both STIM1 and STIM2 severely impairs cytokine production (41, 76, 77). We were therefore surprised to find normal expression of IL-2, IL-6, IL-10, IL-12p70, IL-12/23p40 and TNFα in STIM1/STIM2-deficient BMDMs and BMDCs following stimulation with a variety of different PRR ligands that had been linked to Ca^{2+} signals (**Figure 8**) (27-30, 32-34, 61, 63, 65). Curdlan and zymosan are beta glucans binding to the Dectin-1 receptor, which activates PLCγ2 via the kinase Syk (34). The resulting IP_3 production is thought to trigger a transient Ca^{2+} release from ER stores and thus potentially SOCE (**Figure 8**)(34). We observed Ca^{2+} influx in WT BMDCs after zymosan but not curdlan stimulation that appeared reduced in STIM1/STIM2-deficient cells. Cytokine production in response to zymosan and curdlan, however, was not impaired. LPS binds to TLR4 and CD14 and was shown to induce Ca^{2+} signals in murine BMDCs (29, 30, 35, 65). The LPS-induced expression of TNFα and IL-6 was attenuated by non-selective inhibition of Ca^{2+} channels with SKF-96365 (35). We found only a weak LPS-induced Ca^{2+} response in a small fraction of WT BMDCs, which appeared absent in STIM1/STIM2-deficient cells. However, we did not observe significant defects in LPS-induced cytokine production in STIM1/STIM2-deficient DCs and macrophages. These findings are in contrast to impaired expression of IL-10, IL-12 and IFNγ after LPS stimulation of human monocyte-derived DCs in the presence of 2-APB (36). 2-APB, however, is a non-selective modulator of several ion channels. It not only modulates CRAC

channel function and SOCE (57, 78), but also that of TRPV channels (58, 79, 80), TRPM channels (81), TRPC channels (81), the potassium channel KCa3.1 that is expressed in macrophages (81, 82), $GABA_A$ receptors (83) and IP3Rs (reviewed in (84)). 2-APB therefore has much broader effects on Ca^{2+} signaling than the inhibition of SOCE alone. While our data do not contradict a role of Ca^{2+} signals in the regulation of cytokine expression in macrophages and DCs, they argue against an essential role of SOCE in cytokine production following PRR engagement.

Extracellular Ca^{2+} as a danger signal was recently shown to be required for the assembly and activation of the NLRP3 inflammasome following binding to CASR on the cell surface (39, 40). Ca^{2+} influx reportedly mediates activation of the NLRP3 inflammasome because the non-selective ion channel inhibitor 2-APB blunted IL-1β secretion (38). This is consistent with our findings of a moderate reduction in NLRP3 activation when BMDMs were stimulated in the presence of 2-APB and, more strikingly, abolished NLRP3 activation when intracellular Ca^{2+} was chelated with BAPTA. Removal of extracellular Ca^{2+} with EGTA, however, had almost no effect on IL-1β secretion and STIM1/STIM2-deficient BMDMs showed normal caspase 1 cleavage and subsequent IL-1β release. Because 2-APB non-selectively modulates many ion channels besides CRAC channels as discussed above, and BAPTA suppresses all intracellular Ca^{2+} signaling, these data collectively suggest that Ca^{2+} signals (potentially mediated by P2X7 receptors or Ca^{2+} release from ER stores) but not SOCE are required for NLRP3 inflammasome activation. Given recent reports that K^+ efflux but not Ca^{2+} influx is essential for NLRP3 activation (85, 86) further studies if and how Ca^{2+} signaling exactly contributes to NLRP3 inflammasome activation are required.

Ca^{2+} signals have been implicated in the development and function of DCs in response to microbial pathogens, and may thus play an important role in regulating innate immunity (31). This view is supported by experiments in which enforcing Ca^{2+} signaling in DCs with Ca^{2+} ionophores promoted DC maturation whereas chelation of intracellular Ca^{2+} inhibited DC maturation (25, 36, 71). However, these experimental procedures are very artificial and the Ca^{2+} signaling pathways that regulate DC development and function under more physiological conditions remain unknown. Two studies have reported Ca^{2+} currents in DCs that resemble CRAC channel currents in T cells and observed that stimulation of DC with IP_3 or LPS induces SOCE (25, 35). Direct evidence for a role of SOCE in DCs comes from human monocyte-derived DC in which siRNA mediated knockdown of STIM1 or ORAI1 expression prevented LPS and TNFα induced maturation of DC *in vitro* (36). Whether SOCE is also required for other DC functions such as antigen presentation or inflammasome activation and especially for their function *in vivo* remained unclear. We found that deletion of STIM1 and STIM2 completely abolishes SOCE in BMDCs. Surprisingly however, the differentiation and maturation of DCs in response to a variety of TLR and other PRR ligands was unperturbed. Likewise, STIM1/STIM2-deficient DCs incubated with ovalbumin were able to induce proliferation and IFNγ production of cognate T cells, suggesting that none of the steps required for antigen presentation by DCs (including antigen uptake, processing and loading onto MHC class II as well as expression of co-stimulatory molecules and cytokines) was significantly impaired in the absence of STIM1 and STIM2. By contrast, chelating

$[Ca^{2+}]_i$ with BAPTA significantly reduced T cell activation, suggesting that intracellular Ca^{2+} signals but not SOCE are required for the APC function of DCs.

STIM1 and STIM2 mediate SOCE in macrophages and DC but their deletion and subsequent complete suppression of SOCE has no effects on the function of these cells. At present, we cannot exclude that the SOCE-independent function of macrophages and DC is specific to in vitro-differentiated BMDMs and BMDCs and that particular functions of primary macrophages and DC *in vivo* are dependent on SOCE. It is noteworthy, however, that peritoneal macrophages isolated from STIM1/STIM2-deficient mice showed no defect in the phagocytosis of opsonized RBCs. In addition, $CD11b^+$ and $CD11c^+$ DC isolated from MOG-immunized *Stim1*$^{-/-}$ BM chimeric mice and *Stim2*$^{-/-}$ mice showed normal expression of costimulatory receptors MHCII, CD80, CD86 and CD40 and were able to activate MOG-specific T cells *in vitro* (87), suggesting that STIM1 and STIM2 alone are not required for the antigen presenting function of DCs. Future studies using mice with macrophage and DC-specific deletion of *Stim1* and *Stim2* genes will have to address the role of SOCE in innate immune responses in vivo.

Our studies demonstrate that whereas intracellular Ca^{2+} signals are required for several innate immune functions of macrophages and DCs, SOCE mediated by STIM1 and STIM2 is dispensable for these processes. This is in contrast to the important role of SOCE in T cells and their ability to provide immunity to infection (9, 10) and to mediate inflammation in the context of autoimmunity (47, 76, 87). Genetic or pharmacological inhibition of SOCE in lymphocytes prevents T cell mediated autoimmunity and inflammation in preclinical models of diseases such as multiple sclerosis (76, 87), inflammatory bowel disease (47), skin allograft rejection (47) and allergic asthma (88), which may be utilized for the treatment of diseases in human patients. The beneficial effects of CRAC channel inhibition on pro-inflammatory T cells need to be balanced, however, against their immunosuppressive effects that result in increased susceptibility to infection. As CRAC channel inhibitors are under development to treat autoimmune and inflammatory diseases, the dispensable role of SOCE in macrophages and DCs that we found in this study suggests that selective CRAC channel inhibitors are unlikely to have significant side effects on innate immunity.

Supplementary Material

Refer to Web version on PubMed Central for supplementary material.

Acknowledgements

We thank Dr. Russell Vance (University of California, Berkeley) for providing the FlaTox reagent and Dr. Victor Torres (NYU School of Medicine) for GFP-expressing *S. aureus*. $CD45.1^+$ congenic $OT\text{-}II^+$ mice were a gift from Dr. Adrian Erlebacher (NYU School of Medicine) and the CMG14-12 cell line was provided by Dr. Ken Cadwell (NYU School of Medicine). We are grateful to Dr. Masatsugu Oh-hora (Kyushu University, Japan) for his generous help with *Stim1*$^{fl/fl}$*Stim2*$^{fl/fl}$ *Vav-Cre* and *Stim1*$^{fl/fl}$*Stim2*$^{fl/fl}$ *Mx1-Cre* mice after hurricane Sandy decimated our mouse colony.

This work was funded by NIH grants AI097302 to S.F., AI065303 to D.U., AI087682 to J.P. and postdoctoral fellowships by the National Multiple Sclerosis Society to P.S, the Alfonso Martin Escudero foundation to A.R.C. and the Deutsche Forschungsgemeinschaft (DFG) to C.W. (We 5303/1-1) and M.V. (VA 882/1-1).

References

1. Feske S, Wulff H, Skolnik EY. Ion channels in innate and adaptive immunity. Annu Rev Immunol. 2014 in press.
2. Feske S, Gwack Y, Prakriya M, Srikanth S, Puppel SH, Tanasa B, Hogan PG, Lewis RS, Daly M, Rao A. A mutation in Orai1 causes immune deficiency by abrogating CRAC channel function. Nature. 2006; 441:179–185. [PubMed: 16582901]
3. Vig M, Peinelt C, Beck A, Koomoa DL, Rabah D, Koblan-Huberson M, Kraft S, Turner H, Fleig A, Penner R, Kinet JP. CRACM1 is a plasma membrane protein essential for store-operated Ca2+ entry. Science. 2006; 312:1220–1223. [PubMed: 16645049]
4. Zhang SL, Yeromin AV, Zhang XH, Yu Y, Safrina O, Penna A, Roos J, Stauderman KA, Cahalan MD. Genome-wide RNAi screen of Ca(2+) influx identifies genes that regulate Ca(2+) release-activated Ca(2+) channel activity. Proceedings of the National Academy of Sciences of the United States of America. 2006; 103:9357–9362. [PubMed: 16751269]
5. Shaw PJ, Qu B, Hoth M, Feske S. Molecular regulation of CRAC channels and their role in lymphocyte function. Cellular and molecular life sciences : CMLS. 2013; 70:2637–2656. [PubMed: 23052215]
6. Feske S. Immunodeficiency due to defects in store-operated calcium entry. Annals of the New York Academy of Sciences. 2011; 1238:74–90. [PubMed: 22129055]
7. McCarl CA, Picard C, Khalil S, Kawasaki T, Rother J, Papolos A, Kutok J, Hivroz C, Ledeist F, Plogmann K, Ehl S, Notheis G, Albert MH, Belohradsky BH, Kirschner J, Rao A, Fischer A, Feske S. ORAI1 deficiency and lack of store-operated Ca2+ entry cause immunodeficiency, myopathy, and ectodermal dysplasia. J Allergy Clin Immunol. 2009; 124:1311–1318 e1317. [PubMed: 20004786]
8. Picard C, McCarl CA, Papolos A, Khalil S, Luthy K, Hivroz C, LeDeist F, Rieux-Laucat F, Rechavi G, Rao A, Fischer A, Feske S. STIM1 mutation associated with a syndrome of immunodeficiency and autoimmunity. The New England journal of medicine. 2009; 360:1971–1980. [PubMed: 19420366]
9. Desvignes L, Weidinger C, Shaw PJ, Vaeth M, Ribierre T, Liu M, Fergus T, Kozhaya L, McVoy L, Unutmaz D, Ernst JD, Feske S. STIM1 controls T cell-mediated immune regulation and inflammation in chronic infection. Journal of Clinical Investigation. 2015 [in press].
10. Shaw PJ, Weidinger C, Vaeth M, Luethy K, Kaech SM, Feske S. CD4+ and CD8+ T cell-dependent antiviral immunity requires STIM1 and STIM2. The Journal of clinical investigation. 2014; 124:4549–4563. [PubMed: 25157823]
11. Chen BC, Chou CF, Lin WW. Pyrimidinoceptor-mediated potentiation of inducible nitric-oxide synthase induction in J774 macrophages. Role of intracellular calcium. J Biol Chem. 1998; 273:29754–29763. [PubMed: 9792689]
12. Watanabe N, Suzuki J, Kobayashi Y. Role of calcium in tumor necrosis factor-alpha production by activated macrophages. J Biochem. 1996; 120:1190–1195. [PubMed: 9010769]
13. Di Virgilio F, Meyer BC, Greenberg S, Silverstein SC. Fc receptor-mediated phagocytosis occurs in macrophages at exceedingly low cytosolic Ca2+ levels. J Cell Biol. 1988; 106:657–666. [PubMed: 3346321]
14. Greenberg S, el Khoury J, di Virgilio F, Kaplan EM, Silverstein SC. Ca(2+)-independent F-actin assembly and disassembly during Fc receptor-mediated phagocytosis in mouse macrophages. J Cell Biol. 1991; 113:757–767. [PubMed: 2026648]
15. Hishikawa T, Cheung JY, Yelamarty RV, Knutson DW. Calcium transients during Fc receptor-mediated and nonspecific phagocytosis by murine peritoneal macrophages. J Cell Biol. 1991; 115:59–66. [PubMed: 1918139]
16. Young JD, Ko SS, Cohn ZA. The increase in intracellular free calcium associated with IgG gamma 2b/gamma 1 Fc receptor-ligand interactions: role in phagocytosis. Proceedings of the National Academy of Sciences of the United States of America. 1984; 81:5430–5434. [PubMed: 6236462]
17. McNeil PL, Swanson JA, Wright SD, Silverstein SC, Taylor DL. Fc-receptor-mediated phagocytosis occurs in macrophages without an increase in average [Ca++]i. J Cell Biol. 1986; 102:1586–1592. [PubMed: 3700467]

18. Braun A, Gessner JE, Varga-Szabo D, Syed SN, Konrad S, Stegner D, Vogtle T, Schmidt RE, Nieswandt B. STIM1 is essential for Fcgamma receptor activation and autoimmune inflammation. Blood. 2009; 113:1097–1104. [PubMed: 18941110]
19. Kusner DJ, Barton JA. ATP stimulates human macrophages to kill intracellular virulent Mycobacterium tuberculosis via calcium-dependent phagosome-lysosome fusion. J Immunol. 2001; 167:3308–3315. [PubMed: 11544319]
20. Malik ZA, Denning GM, Kusner DJ. Inhibition of Ca(2+) signaling by Mycobacterium tuberculosis is associated with reduced phagosome-lysosome fusion and increased survival within human macrophages. The Journal of experimental medicine. 2000; 191:287–302. [PubMed: 10637273]
21. Vergne I, Chua J, Deretic V. Tuberculosis toxin blocking phagosome maturation inhibits a novel Ca2+/calmodulin-PI3K hVPS34 cascade. The Journal of experimental medicine. 2003; 198:653–659. [PubMed: 12925680]
22. Jayachandran R, Sundaramurthy V, Combaluzier B, Mueller P, Korf H, Huygen K, Miyazaki T, Albrecht I, Massner J, Pieters J. Survival of mycobacteria in macrophages is mediated by coronin 1-dependent activation of calcineurin. Cell. 2007; 130:37–50. [PubMed: 17632055]
23. Zimmerli S, Majeed M, Gustavsson M, Stendahl O, Sanan DA, Ernst JD. Phagosome-lysosome fusion is a calcium-independent event in macrophages. J Cell Biol. 1996; 132:49–61. [PubMed: 8567729]
24. Czerniecki BJ, Carter C, Rivoltini L, Koski GK, Kim HI, Weng DE, Roros JG, Hijazi YM, Xu S, Rosenberg SA, Cohen PA. Calcium ionophore-treated peripheral blood monocytes and dendritic cells rapidly display characteristics of activated dendritic cells. J Immunol. 1997; 159:3823–3837. [PubMed: 9378970]
25. Hsu S, O'Connell PJ, Klyachko VA, Badminton MN, Thomson AW, Jackson MB, Clapham DE, Ahern GP. Fundamental Ca2+ signaling mechanisms in mouse dendritic cells: CRAC is the major Ca2+ entry pathway. J Immunol. 2001; 166:6126–6133. [PubMed: 11342632]
26. Koski GK, Schwartz GN, Weng DE, Gress RE, Engels FH, Tsokos M, Czerniecki BJ, Cohen PA. Calcium ionophore-treated myeloid cells acquire many dendritic cell characteristics independent of prior differentiation state, transformation status, or sensitivity to biologic agents. Blood. 1999; 94:1359–1371. [PubMed: 10438724]
27. Herbst S, Shah A, Mazon Moya M, Marzola V, Jensen B, Reed A, Birrell MA, Saijo S, Mostowy S, Shaunak S, Armstrong-James D. Phagocytosis-dependent activation of a TLR9-BTK-calcineurin-NFAT pathway co-ordinates innate immunity to Aspergillus fumigatus. EMBO molecular medicine. 2015; 7:240–258. [PubMed: 25637383]
28. Rao S, Liu X, Freedman BD, Behrens EM. Spleen tyrosine kinase (Syk)-dependent calcium signals mediate efficient CpG-induced exocytosis of tumor necrosis factor alpha (TNFalpha) in innate immune cells. J Biol Chem. 2013; 288:12448–12458. [PubMed: 23515313]
29. Zanoni I, Ostuni R, Capuano G, Collini M, Caccia M, Ronchi AE, Rocchetti M, Mingozzi F, Foti M, Chirico G, Costa B, Zaza A, Ricciardi-Castagnoli P, Granucci F. CD14 regulates the dendritic cell life cycle after LPS exposure through NFAT activation. Nature. 2009; 460:264–268. [PubMed: 19525933]
30. Zanoni I, Ostuni R, Marek LR, Barresi S, Barbalat R, Barton GM, Granucci F, Kagan JC. CD14 controls the LPS-induced endocytosis of Toll-like receptor 4. Cell. 2011; 147:868–880. [PubMed: 22078883]
31. Connolly SF, Kusner DJ. The regulation of dendritic cell function by calcium- signaling and its inhibition by microbial pathogens. Immunol Res. 2007; 39:115–127. [PubMed: 17917060]
32. Kelly EK, Wang L, Ivashkiv LB. Calcium-activated pathways and oxidative burst mediate zymosan-induced signaling and IL-10 production in human macrophages. J Immunol. 2010; 184:5545–5552. [PubMed: 20400701]
33. Goodridge HS, Simmons RM, Underhill DM. Dectin-1 stimulation by Candida albicans yeast or zymosan triggers NFAT activation in macrophages and dendritic cells. J Immunol. 2007; 178:3107–3115. [PubMed: 17312158]

34. Xu S, Huo J, Lee KG, Kurosaki T, Lam KP. Phospholipase Cgamma2 is critical for Dectin-1-mediated Ca2+ flux and cytokine production in dendritic cells. J Biol Chem. 2009; 284:7038–7046. [PubMed: 19136564]
35. Matzner N, Zemtsova IM, Nguyen TX, Duszenko M, Shumilina E, Lang F. Ion channels modulating mouse dendritic cell functions. J Immunol. 2008; 181:6803–6809. [PubMed: 18981098]
36. Felix R, Crottes D, Delalande A, Fauconnier J, Lebranchu Y, Le Guennec JY, Velge- Roussel F. The Orai-1 and STIM-1 complex controls human dendritic cell maturation. PloS one. 2013; 8:e61595. [PubMed: 23700407]
37. Schroder K, Tschopp J. The inflammasomes. Cell. 2010; 140:821–832. [PubMed: 20303873]
38. Murakami T, Ockinger J, Yu J, Byles V, McColl A, Hofer AM, Horng T. Critical role for calcium mobilization in activation of the NLRP3 inflammasome. Proceedings of the National Academy of Sciences of the United States of America. 2012; 109:11282–11287. [PubMed: 22733741]
39. Lee GS, Subramanian N, Kim AI, Aksentijevich I, Goldbach-Mansky R, Sacks DB, Germain RN, Kastner DL, Chae JJ. The calcium-sensing receptor regulates the NLRP3 inflammasome through Ca2+ and cAMP. Nature. 2012; 492:123–127. [PubMed: 23143333]
40. Rossol M, Pierer M, Raulien N, Quandt D, Meusch U, Rothe K, Schubert K, Schoneberg T, Schaefer M, Krugel U, Smajilovic S, Brauner-Osborne H, Baerwald C, Wagner U. Extracellular Ca2+ is a danger signal activating the NLRP3 inflammasome through G protein- coupled calcium sensing receptors. Nature communications. 2012; 3:1329.
41. Oh-Hora M, Yamashita M, Hogan PG, Sharma S, Lamperti E, Chung W, Prakriya M, Feske S, Rao A. Dual functions for the endoplasmic reticulum calcium sensors STIM1 and STIM2 in T cell activation and tolerance. Nature immunology. 2008; 9:432–443. [PubMed: 18327260]
42. Oh-Hora M, Komatsu N, Pishyareh M, Feske S, Hori S, Taniguchi M, Rao A, Takayanagi H. Agonist-selected T cell development requires strong T cell receptor signaling and store-operated calcium entry. Immunity. 2013; 38:881–895. [PubMed: 23499491]
43. Kuhn R, Schwenk F, Aguet M, Rajewsky K. Inducible gene targeting in mice. Science. 1995; 269:1427–1429. [PubMed: 7660125]
44. Takeshita S, Kaji K, Kudo A. Identification and characterization of the new osteoclast progenitor with macrophage phenotypes being able to differentiate into mature osteoclasts. Journal of bone and mineral research : the official journal of the American Society for Bone and Mineral Research. 2000; 15:1477–1488.
45. Mehra A, Zahra A, Thompson V, Sirisaengtaksin N, Wells A, Porto M, Koster S, Penberthy K, Kubota Y, Dricot A, Rogan D, Vidal M, Hill DE, Bean AJ, Philips JA. Mycobacterium tuberculosis type VII secreted effector EsxH targets host ESCRT to impair trafficking. PLoS pathogens. 2013; 9:e1003734. [PubMed: 24204276]
46. Lutz MB, Kukutsch N, Ogilvie AL, Rossner S, Koch F, Romani N, Schuler G. An advanced culture method for generating large quantities of highly pure dendritic cells from mouse bone marrow. Journal of immunological methods. 1999; 223:77–92. [PubMed: 10037236]
47. McCarl CA, Khalil S, Ma J, Oh-hora M, Yamashita M, Roether J, Kawasaki T, Jairaman A, Sasaki Y, Prakriya M, Feske S. Store-operated Ca2+ entry through ORAI1 is critical for T cell-mediated autoimmunity and allograft rejection. J Immunol. 2010; 185:5845–5858. [PubMed: 20956344]
48. Weidinger C, Shaw PJ, Feske S. STIM1 and STIM2-mediated Ca(2+) influx regulates antitumour immunity by CD8(+) T cells. EMBO molecular medicine. 2013; 5:1311–1321. [PubMed: 23922331]
49. DuMont AL, Yoong P, Day CJ, Alonzo F 3rd, McDonald WH, Jennings MP, Torres VJ. Staphylococcus aureus LukAB cytotoxin kills human neutrophils by targeting the CD11b subunit of the integrin Mac-1. Proceedings of the National Academy of Sciences of the United States of America. 2013; 110:10794–10799. [PubMed: 23754403]
50. Zhang H, Clemens RA, Liu F, Hu Y, Baba Y, Theodore P, Kurosaki T, Lowell CA. STIM1 calcium sensor is required for activation of the phagocyte oxidase during inflammation and host defense. Blood. 2014; 123:2238–2249. [PubMed: 24493668]

51. Le Deist F, Hivroz C, Partiseti M, Thomas C, Buc HA, Oleastro M, Belohradsky B, Choquet D, Fischer A. A primary T-cell immunodeficiency associated with defective transmembrane calcium influx. Blood. 1995; 85:1053–1062. [PubMed: 7531512]
52. von Moltke J, Trinidad NJ, Moayeri M, Kintzer AF, Wang SB, van Rooijen N, Brown CR, Krantz BA, Leppla SH, Gronert K, Vance RE. Rapid induction of inflammatory lipid mediators by the inflammasome in vivo. Nature. 2012; 490:107–111. [PubMed: 22902502]
53. Brough D, Le Feuvre RA, Wheeler RD, Solovyova N, Hilfiker S, Rothwell NJ, Verkhratsky A. Ca2+ stores and Ca2+ entry differentially contribute to the release of IL-1 beta and IL-1 alpha from murine macrophages. J Immunol. 2003; 170:3029–3036. [PubMed: 12626557]
54. Horng T. Calcium signaling and mitochondrial destabilization in the triggering of the NLRP3 inflammasome. Trends in immunology. 2014; 35:253–261. [PubMed: 24646829]
55. de Boer J, Williams A, Skavdis G, Harker N, Coles M, Tolaini M, Norton T, Williams K, Roderick K, Potocnik AJ, Kioussis D. Transgenic mice with hematopoietic and lymphoid specific expression of Cre. European journal of immunology. 2003; 33:314–325. [PubMed: 12548562]
56. Bandyopadhyay BC, Pingle SC, Ahern GP. Store-operated Ca(2)+ signaling in dendritic cells occurs independently of STIM1. Journal of leukocyte biology. 2011; 89:57–62. [PubMed: 20971921]
57. Hendron E, Wang X, Zhou Y, Cai X, Goto J, Mikoshiba K, Baba Y, Kurosaki T, Wang Y, Gill DL. Potent functional uncoupling between STIM1 and Orai1 by dimeric 2- aminodiphenyl borinate analogs. Cell calcium. 2014; 56:482–492.. [PubMed: 25459299]
58. Voets T, Prenen J, Fleig A, Vennekens R, Watanabe H, Hoenderop JG, Bindels RJ, Droogmans G, Penner R, Nilius B. CaT1 and the calcium release-activated calcium channel manifest distinct pore properties. J Biol Chem. 2001; 276:47767–47770. [PubMed: 11687570]
59. Bootman MD, Collins TJ, Mackenzie L, Roderick HL, Berridge MJ, Peppiatt CM. 2-aminoethoxydiphenyl borate (2-APB) is a reliable blocker of store-operated Ca2+ entry but an inconsistent inhibitor of InsP3-induced Ca2+ release. FASEB journal : official publication of the Federation of American Societies for Experimental Biology. 2002; 16:1145–1150. [PubMed: 12153982]
60. Colton CK, Zhu MX. 2-Aminoethoxydiphenyl borate as a common activator of TRPV1, TRPV2, and TRPV3 channels. Handbook of experimental pharmacology. 2007:173–187. [PubMed: 17217057]
61. Granucci F, Zanoni I. The dendritic cell life cycle. Cell cycle. 2009; 8:3816–3821. [PubMed: 19887908]
62. Hwang H, Min H, Kim D, Yu SW, Jung SJ, Choi SY, Lee SJ. Imiquimod induces a Toll-like receptor 7-independent increase in intracellular calcium via IP(3) receptor activation. Biochemical and biophysical research communications. 2014; 450:875–879. [PubMed: 24971541]
63. Dominguez-Villar M, Gautron AS, de Marcken M, Keller MJ, Hafler DA. TLR7 induces anergy in human CD4(+) T cells. Nature immunology. 2015; 16:118–128. [PubMed: 25401424]
64. Feske S. Calcium signalling in lymphocyte activation and disease. Nature reviews. Immunology. 2007; 7:690–702.
65. Zanoni I, Ostuni R, Barresi S, Di Gioia M, Broggi A, Costa B, Marzi R, Granucci F. CD14 and NFAT mediate lipopolysaccharide-induced skin edema formation in mice. The Journal of clinical investigation. 2012; 122:1747–1757. [PubMed: 22466648]
66. Zanoni I, Granucci F. Regulation and dysregulation of innate immunity by NFAT signaling downstream of pattern recognition receptors (PRRs). European journal of immunology. 2012; 42:1924–1931. [PubMed: 22706795]
67. Greenblatt MB, Aliprantis A, Hu B, Glimcher LH. Calcineurin regulates innate antifungal immunity in neutrophils. J Exp Med. 2010; 207:923–931. [PubMed: 20421389]
68. Chu J, Thomas LM, Watkins SC, Franchi L, Nunez G, Salter RD. Cholesterol- dependent cytolysins induce rapid release of mature IL-1beta from murine macrophages in a NLRP3 inflammasome and cathepsin B-dependent manner. Journal of leukocyte biology. 2009; 86:1227–1238. [PubMed: 19675207]

69. Feldmeyer L, Keller M, Niklaus G, Hohl D, Werner S, Beer HD. The inflammasome mediates UVB-induced activation and secretion of interleukin-1beta by keratinocytes. Current biology : CB. 2007; 17:1140–1145. [PubMed: 17600714]
70. Hanley PJ, Kronlage M, Kirschning C, del Rey A, Di Virgilio F, Leipziger J, Chessell IP, Sargin S, Filippov MA, Lindemann O, Mohr S, Konigs V, Schillers H, Bahler M, Schwab A. Transient P2X7 receptor activation triggers macrophage death independent of Toll-like receptors 2 and 4, caspase-1, and pannexin-1 proteins. J Biol Chem. 2012; 287:10650–10663. [PubMed: 22235111]
71. Shumilina E, Huber SM, Lang F. Ca2+ signaling in the regulation of dendritic cell functions. American journal of physiology. Cell physiology. 2011; 300:C1205–1214. [PubMed: 21451105]
72. Fuchs S, Rensing-Ehl A, Speckmann C, Bengsch B, Schmitt-Graeff A, Bondzio I, Maul- Pavicic A, Bass T, Vraetz T, Strahm B, Ankermann T, Benson M, Caliebe A, Folster-Holst R, Kaiser P, Thimme R, Schamel WW, Schwarz K, Feske S, Ehl S. Antiviral and regulatory T cell immunity in a patient with stromal interaction molecule 1 deficiency. J Immunol. 2012; 188:1523–1533. [PubMed: 22190180]
73. Matsumoto M, Fujii Y, Baba A, Hikida M, Kurosaki T, Baba Y. The calcium sensors STIM1 and STIM2 control B cell regulatory function through interleukin-10 production. Immunity. 2011; 34:703–714. [PubMed: 21530328]
74. Nuvolone M, Kana V, Hutter G, Sakata D, Mortin-Toth SM, Russo G, Danska JS, Aguzzi A. SIRPalpha polymorphisms, but not the prion protein, control phagocytosis of apoptotic cells. J Exp Med. 2013; 210:2539–2552. [PubMed: 24145514]
75. Wen AY, Sakamoto KM, Miller LS. The role of the transcription factor CREB in immune function. J Immunol. 2010; 185:6413–6419. [PubMed: 21084670]
76. Ma J, McCarl CA, Khalil S, Luthy K, Feske S. T-cell-specific deletion of STIM1 and STIM2 protects mice from EAE by impairing the effector functions of Th1 and Th17 cells. European journal of immunology. 2010; 40:3028–3042. [PubMed: 21061435]
77. Feske S, Draeger R, Peter HH, Eichmann K, Rao A. The duration of nuclear residence of NFAT determines the pattern of cytokine expression in human SCID T cells. J Immunol. 2000; 165:297–305. [PubMed: 10861065]
78. Prakriya M, Lewis RS. Potentiation and inhibition of Ca(2+) release-activated Ca(2+) channels by 2-aminoethyldiphenyl borate (2-APB) occurs independently of IP(3) receptors. The Journal of physiology. 2001; 536:3–19. [PubMed: 11579153]
79. Kovacs G, Montalbetti N, Simonin A, Danko T, Balazs B, Zsembery A, Hediger MA. Inhibition of the human epithelial calcium channel TRPV6 by 2-aminoethoxydiphenyl borate (2-APB). Cell calcium. 2012; 52:468–480. [PubMed: 23040501]
80. Hu HZ, Gu Q, Wang C, Colton CK, Tang J, Kinoshita-Kawada M, Lee LY, Wood JD, Zhu MX. 2-aminoethoxydiphenyl borate is a common activator of TRPV1, TRPV2, and TRPV3. J Biol Chem. 2004; 279:35741–35748. [PubMed: 15194687]
81. Li M, Jiang J, Yue L. Functional characterization of homo- and heteromeric channel kinases TRPM6 and TRPM7. The Journal of general physiology. 2006; 127:525–537.2151519. [PubMed: 16636202]
82. Gao YD, Hanley PJ, Rinne S, Zuzarte M, Daut J. Calcium-activated K(+) channel (K(Ca)3.1) activity during Ca(2+) store depletion and store-operated Ca(2+) entry in human macrophages. Cell calcium. 2010; 48:19–27. [PubMed: 20630587]
83. Rae MG, Hilton J, Sharkey J. Putative TRP channel antagonists, SKF 96365, flufenamic acid and 2-APB, are non-competitive antagonists at recombinant human alpha1beta2gamma2 GABA(A) receptors. Neurochemistry international. 2012; 60:543–554. [PubMed: 22369768]
84. Mikoshiba K. Role of IP3 receptor signaling in cell functions and diseases. Advances in biological regulation. 2015; 57:217–227. [PubMed: 25497594]
85. Katsnelson MA, Rucker LG, Russo HM, Dubyak GR. K+ Efflux Agonists Induce NLRP3 Inflammasome Activation Independently of Ca2+ Signaling. J Immunol. 2015
86. Munoz-Planillo R, Kuffa P, Martinez-Colon G, Smith BL, Rajendiran TM, Nunez G. K(+) efflux is the common trigger of NLRP3 inflammasome activation by bacterial toxins and particulate matter. Immunity. 2013; 38:1142–1153. [PubMed: 23809161]

87. Schuhmann MK, Stegner D, Berna-Erro A, Bittner S, Braun A, Kleinschnitz C, Stoll G, Wiendl H, Meuth SG, Nieswandt B. Stromal interaction molecules 1 and 2 are key regulators of autoreactive T cell activation in murine autoimmune central nervous system inflammation. J Immunol. 2010; 184:1536–1542. [PubMed: 20028655]

88. Yoshino T, Ishikawa J, Ohga K, Morokata T, Takezawa R, Morio H, Okada Y, Honda K, Yamada T. YM-58483, a selective CRAC channel inhibitor, prevents antigen-induced airway eosinophilia and late phase asthmatic responses via Th2 cytokine inhibition in animal models. European journal of pharmacology. 2007; 560:225–233. [PubMed: 17307161]

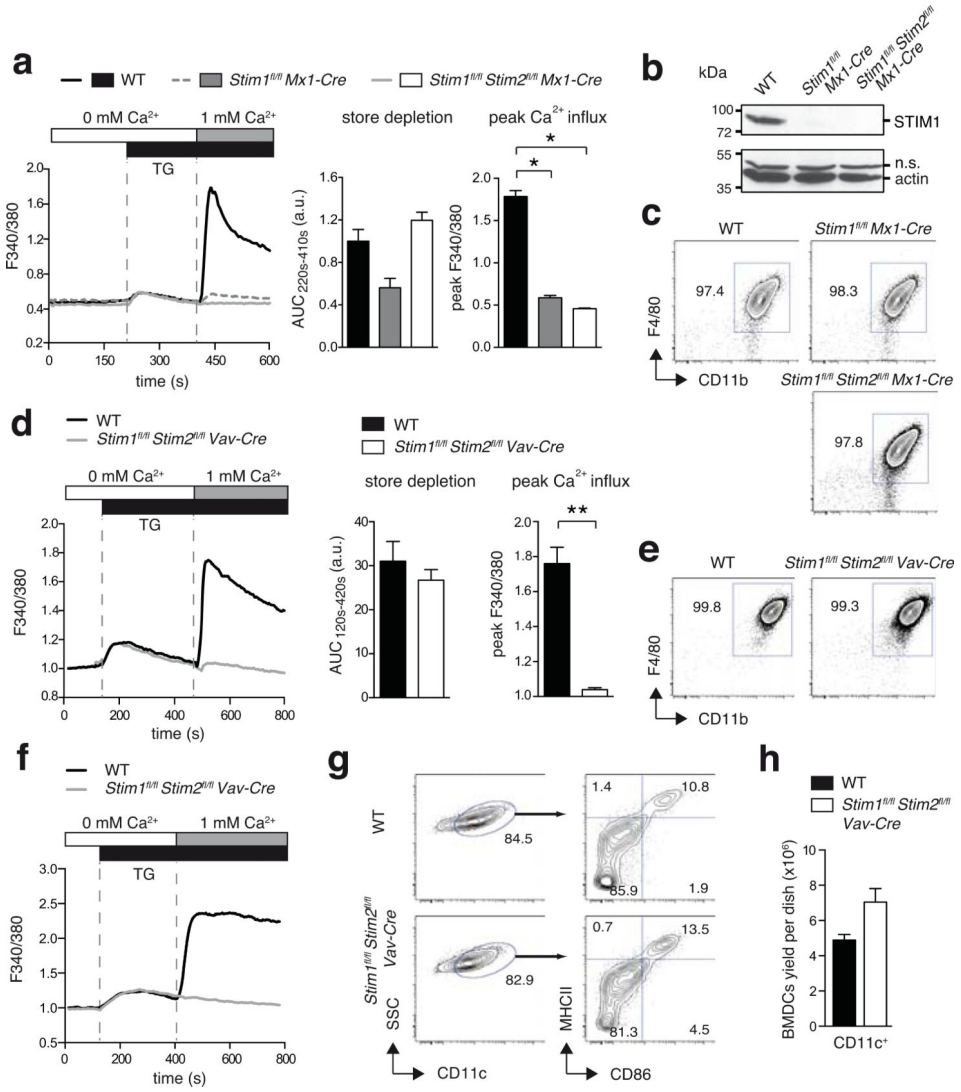

Figure 1. STIM1 and STIM2 are not required for the differentiation of macrophages and DCs

(a-c) Analysis of BMDMs from poly I:C-treated WT, *Stim1$^{fl/fl}$ Mx1-Cre* and *Stim1$^{fl/fl}$Stim2$^{fl/fl}$ Mx1-Cre* mice. (**a**) SOCE in BMDMs was analyzed by time-lapse microscopy. Ca^{2+} store depletion was induced by thapsigargin (TG) stimulation in Ca^{2+}-free buffer and analyzed as the area under the curve ($AUC_{220s\text{-}410s}$); SOCE was induced by readdition of 1 mM extracellular Ca^{2+} and analyzed as peak Ca^{2+} influx. Data represent 3 independent experiments. **(b)** Deletion of STIM1 protein expression. Lysates of BMDMs were separated by SDS-PAGE and incubated with antibodies to STIM1 and Actin. Shown is one representative experiment of 3. n.s., non-specific. **(c)** Phenotypic characterization of BMDMs by flow cytometry. **(d-e)** Analysis of BMDMs differentiated from BM of WT and *Stim1$^{fl/fl}$Stim2$^{fl/fl}$ Vav-Cre* mice. (**d**) SOCE was measured using a FlexStation3 plate reader and analyzed as described in (a). (**e**) Phenotypic characterization of BMDMs was done as described in (c). Data represent 3 independent experiments. **(f-h)** Analysis of BMDCs from WT and *Stim1$^{fl/fl}$Stim2$^{fl/fl}$ Vav-Cre* mice. (**f**) Ca^{2+} store depletion and SOCE in BMDCs were induced as described in (a) and measured using a FlexStation3 plate reader. Graphs

shown are representative of 4 independent experiments. **(g)** Phenotypic characterization of immature BMDCs stained with antibodies to CD11c, CD86, and MHCII and analyzed by flow cytometry. **(h)** Numbers of immature BMDCs after 8 days in culture starting with $2x10^6$ BM cells. Bar graphs represent the mean ± SEM of 9 mice per group. Statistical significance was calculated with an unpaired Student's t test: *, $p<0.05$; **, $p<0.005$.

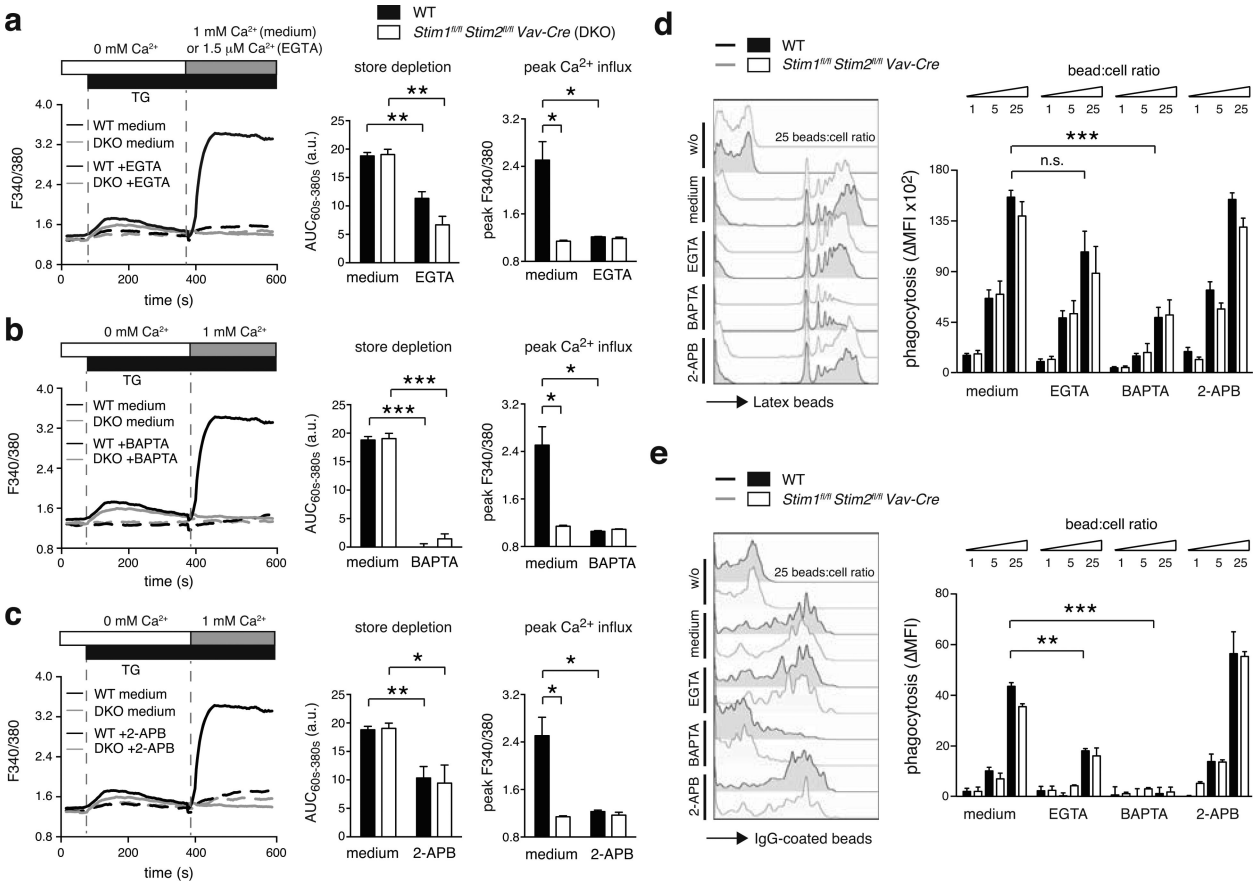

Figure 2. Phagocytosis by BMDMs requires intracellular Ca^{2+} signaling but not SOCE

(a-c) WT and *Stim1*$^{fl/fl}$*Stim2*$^{fl/fl}$ *Vav-Cre* BMDMs were left untreated (medium) or incubated with 2.2 mM EGTA **(a)**, 10 μM BAPTA-AM **(b)**, or 50 μM 2-APB **(c)** for 30 min and $[Ca^{2+}]_i$ was analyzed using a FlexStation3 (ac, left panels). Store depletion ($AUC_{60s\text{-}380s}$) and peak Ca^{2+} influx (peak F340/380) were quantified from 3 individual mice per group (a-c, right panels). **(d,e)** WT and *Stim1*$^{fl/fl}$*Stim2*$^{fl/fl}$ *Vav-Cre* BMDMs were incubated with 1, 5, and 25 bead-to-cell ratios of carboxylate-modified yellow-green microspheres **(d)** or FITC-labeled IgG-coated fluorescent beads **(e)** for 2 h with medium alone or with 2.2 mM EGTA, 10 μM BAPTA-AM, or 50 μM 2-APB as described in (a-c). Phagocytosis was quantified by flow cytometry (left panels) and data from 3 mice per group was compiled as ΔMFI (right panel), where $\Delta MFI = MFI_{beads} - MFI_{no\ beads}$. Bar graphs represent the mean ± SEM. Statistical significance was calculated with an unpaired Student's t test: *, $p<0.05$; **, $p<0.005$; ***, $p<0.001$.

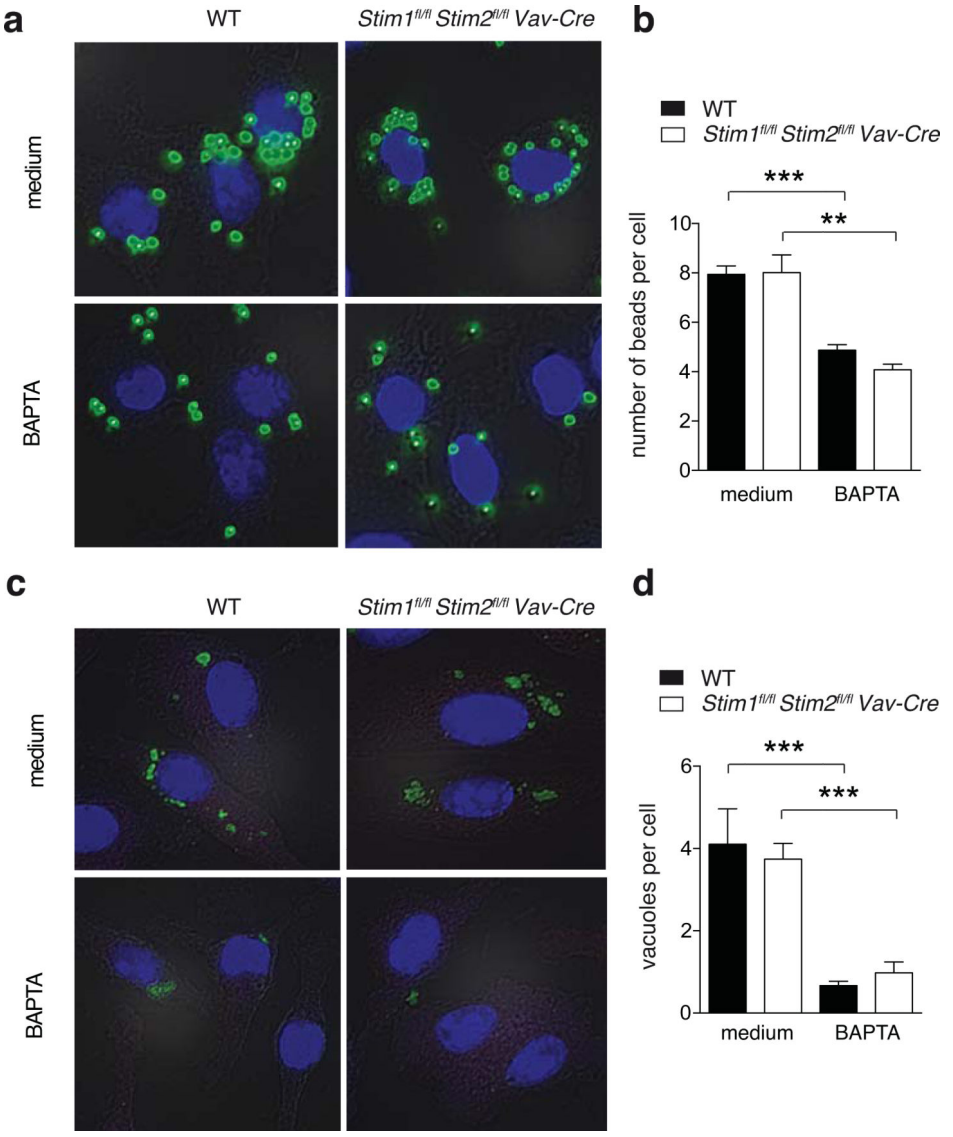

Figure 3. Intracellular Ca^{2+} signaling but not SOCE is required for FcR-dependent and FcR independent phagocytosis in BMDMs

1×10^5 BMDMs from WT and *Stim1$^{fl/fl}$Stim2$^{fl/fl}$ Vav-Cre* mice were treated with 10 μM BAPTA-AM for 30 min or left untreated and incubated with either carboxylate-modified yellow-green microspheres at a 10:1 bead-to-cell ratio **(a,b)** or FITC-labeled IgG-coated beads **(c,d)**. After 30 min, cells were washed 3 times with PBS, fixed and nuclei counterstained with Hoechst 33342 dye. Phagocytosis was analyzed by fluorescence microscopy by measuring the number of beads per cell **(a,b)** or the number of $FITC^+$ vacuoles per cell **(c,d)** from > 50 cells per condition. Bar graphs represent the mean ± SEM. Statistical significance was calculated with an unpaired Student's t test: **, $p<0.01$; ***, $p<0.001$

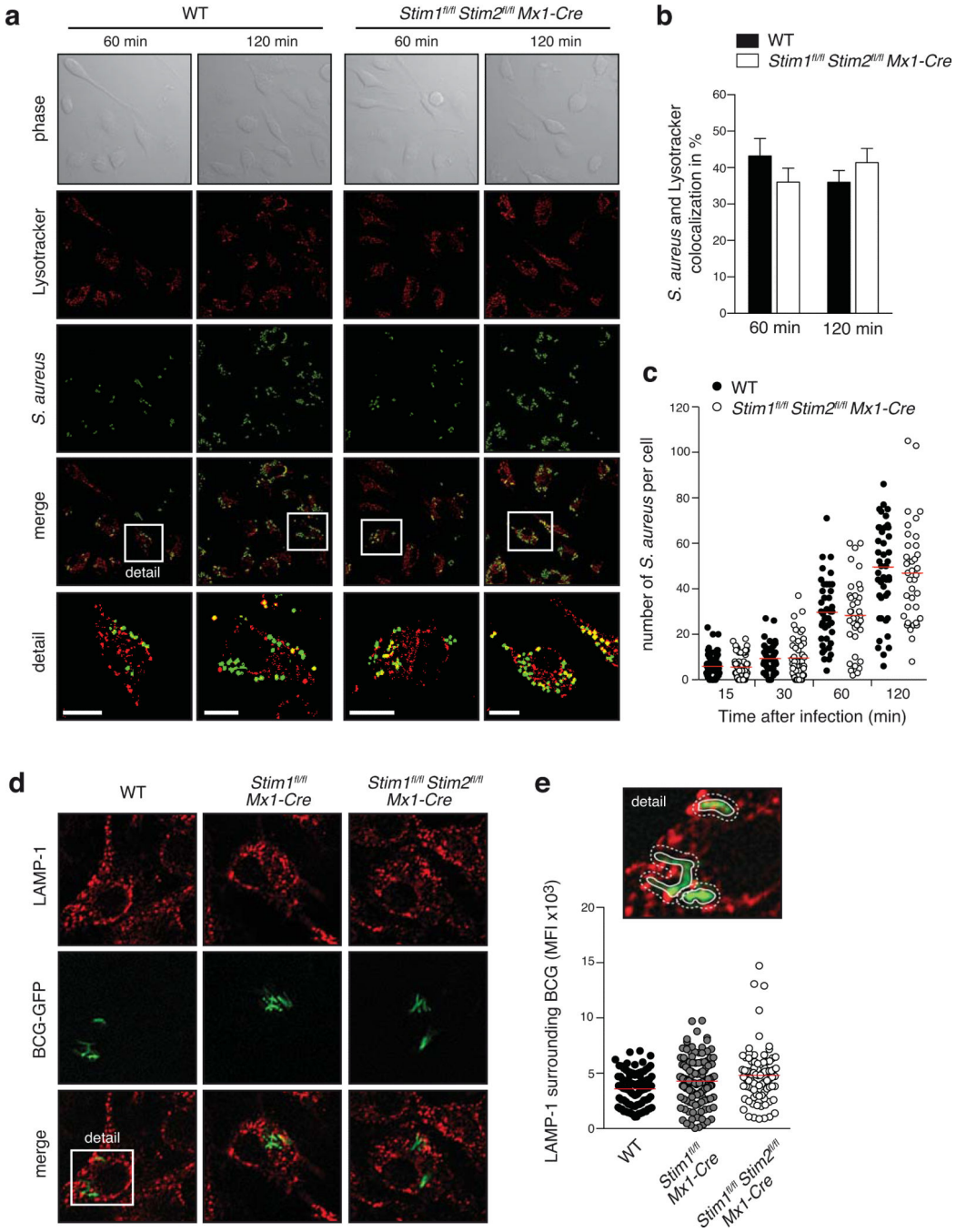

Figure 4. SOCE is not required for lysosomal trafficking of pathogens

(a-c) WT and *Stim1*$^{fl/fl}$*Stim2*$^{fl/fl}$ *Mx1-Cre* BMDMs were incubated with 10 MOI of *S. aureus*-GFP for 2 h. Extracellular *S. aureus* were lysed with Lysostaphin and lysosomes were stained with LysoTracker. **(a)** Representative DIC images of BMDMs, internalized *S. aureus* (green) and LysoTracker (red). Scale bars represent 10 μm. **(b)** Co-localization of internalized *S. aureus* and LysoTracker was quantified after 60 and 120 min by blinded scoring; bar graphs represent mean ± SEM of 4 independent experiments. **(c)** Number of intracellular (phagocytosed) *S. aureus* in individual BMDMs 15, 30, 60, and 120 min after

infection. Each dot represents one cell. **(d-e)** WT, *Stim1*$^{fl/fl}$ *Mx1-Cre* and *Stim1*$^{fl/fl}$*Stim2*$^{fl/fl}$ *Mx1-Cre* BMDMs were infected with 10 MOI of Bacillus Calmette-Guerin-GFP (BCG-GFP) for 3 h before extracellular bacteria were removed. Intracellular trafficking of BCG in BMDMs was measured 24 h later by GFP expression and staining of fixed cells with anti-LAMP-1 antibody. **(d)** Representative confocal microscopy images of internalized BCG-GFP (green) and LAMP-1 (red). **(e)** Quantification of data shown in (d) analyzing the MFI of LAMP-1 in the cell area surrounding BCG (as shown in the example in the upper panel); the quantification represents > 50 cells analyzed from two independent experiments; each dot represents a single intracellular BCG (lower panel).

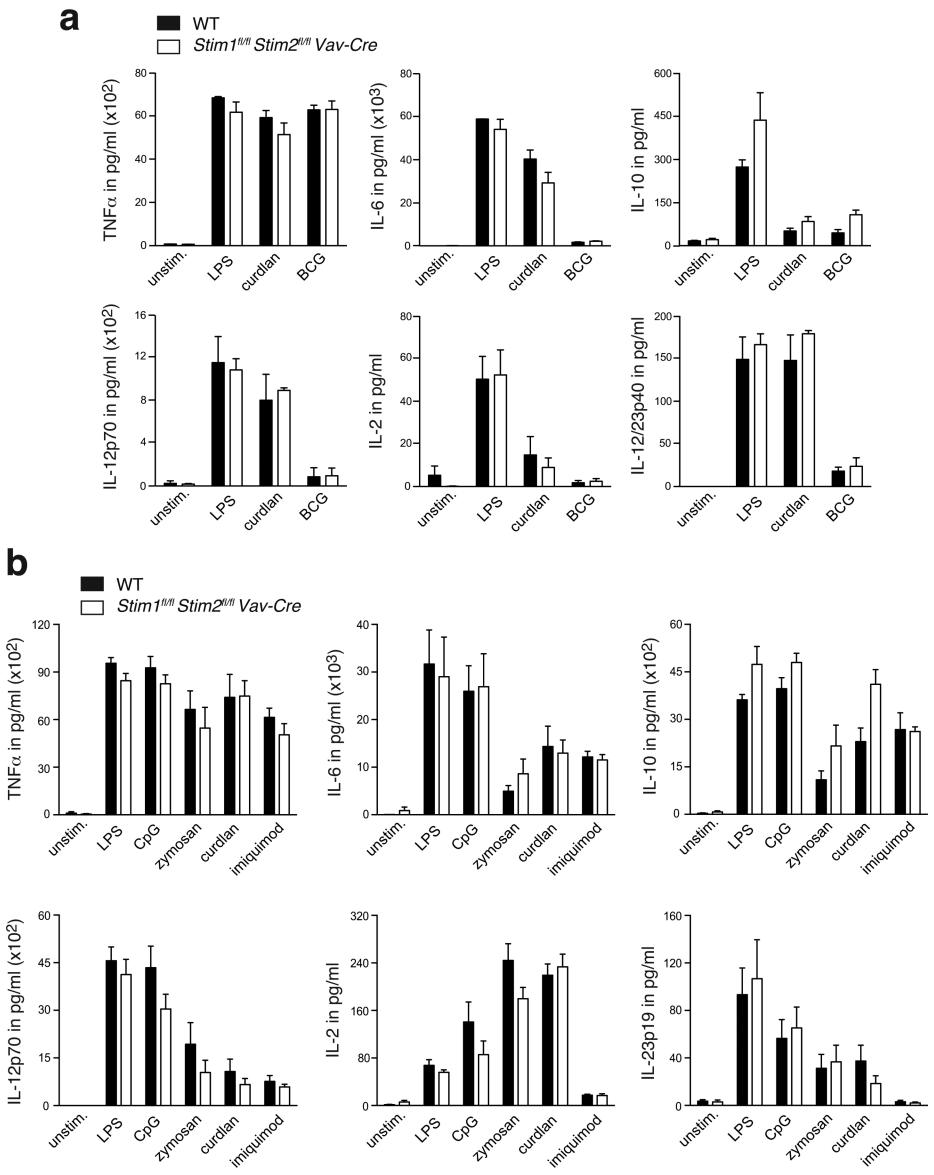

Figure 5. Cytokine production by BMDMs and BMDCs is independent of SOCE

(a) WT and *Stim1*$^{fl/fl}$*Stim2*$^{fl/fl}$ *Vav-Cre* BMDMs were stimulated with 1 μg/ml LPS, 50 μg/ml curdlan, or 5 MOI BCG for 16 h or left untreated (unstim.). Levels of TNFα, IL-6, IL-10, IL-12p70, IL-2, and IL-12/23p40 in the cell supernatant were measured by ELISA. Bar graphs represent the mean ± SEM of 3 mice per group. **(b)** WT and *Stim1*$^{fl/fl}$*Stim2*$^{fl/fl}$ *Vav-Cre* BMDCs were stimulated with 1 μg/ml LPS, 100 nM CpG, 25 μg/ml zymosan, 50 μg/ml curdlan, 1 μg/ml imiquimod for 16 h or left untreated (unstim.). Levels of TNFα, IL-6, IL-10, IL-12p70, IL-2, and IL-23p19 in cell supernatants were analyzed by ELISA. Bar graphs represent the mean ± SEM of 8 mice per group.

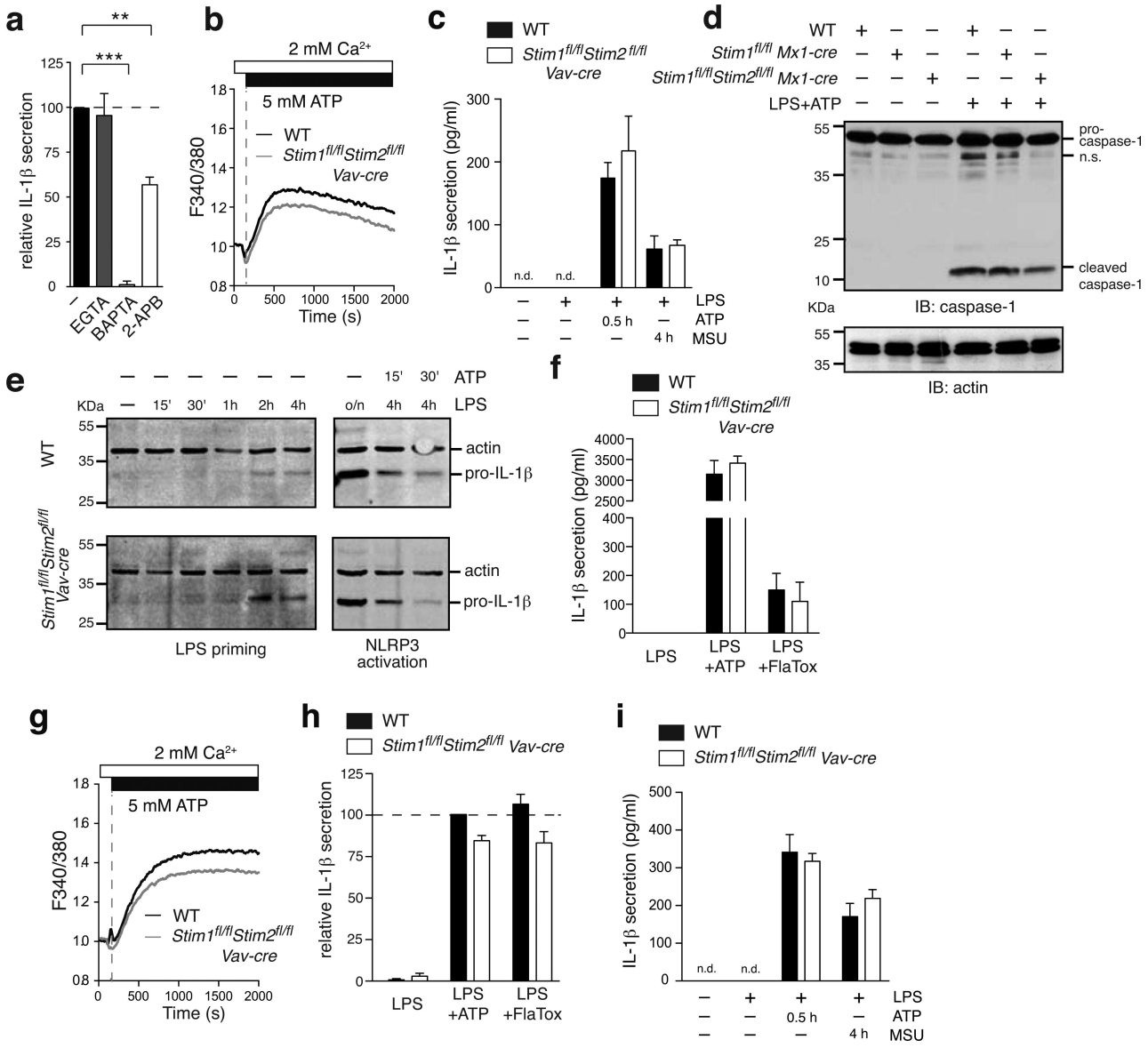

Figure 6. NLRP3 and NLRC4 inflammasome activation does not require STIM1 and STIM2

(a) WT BMDMs were primed for 4 h with 10 μg/ml LPS with or without 2.2 mM EGTA, 10 μM BAPTA-AM or 50 μM 2-APB followed by addition of 3 mM ATP to activate the NLRP3 inflammasome. After 30 min, cell supernatants were analyzed for IL-1β by ELISA. Data are normalized to IL-1β levels in LPS+ATP activated WT BMDMs without inhibition. Bar graphs represent the mean ± SEM from 6 independent experiments. **(b)** Ca^{2+} signals in Fura-2 loaded BMDMs were measured after stimulation with 5 mM ATP in 2 mM Ca^{2+} Ringer solution using a FlexStation3 plate reader. One representative experiment of 2 is shown. **(c)** BMDMs were primed for 4 h with 10 μg/ml LPS followed by stimulation with either 3 mM ATP for 30 min or 150 μg/ml monosodium urate (MSU) crystals for 4 h to activate the NLRP3 inflammasome. Secreted IL-1β in the supernatant was analyzed by ELISA. Bar graphs represent the mean ± SEM of 4 experiments from 2 individual mice per group. n.d.: not detectable. **(d)** BMDMs were left untreated or stimulated with 10 μg/ml LPS

for 4 hours followed by 3 mM ATP for 30 min to activate the NLRP3 inflammasome. Expression levels of pro-caspase-1 (~45 kDa), cleaved caspase-1 (~10 kDa) and actin (loading control) were analyzed by Western blotting. One representative experiment of 3 is shown. n.s., nonspecific. **(e)** BMDMs were primed with 10 μg/ml LPS for 15 min, 30 min, 1 h, 2 h, 4 h and 16 h (o/n) alone or followed after 4 h by stimulation with 3 mM ATP for 15 and 30 min to activate the NLRP3 inflammasome. Intracellular pro-IL-1β (~30 kDa) and actin levels were analyzed in whole cell extracts by Western blotting. **(f)** BMDMs were primed for 4 h with 10 μg/ml LPS followed by stimulation with 3 mM ATP for 30 min to activate the NLRP3 inflammasome or 10 μg/ml LFn-FlaA together with 5 μg/ml PA (referred as FlaTox) to activate the NLRC4 inflammasome. Secreted IL-1β in the supernatant was analyzed by ELISA. Bar graphs represent the mean ± SEM from 4 individual mice per group. **(g-i)** BMDC from WT and *Stim1*$^{fl/fl}$*Stim2*$^{fl/fl}$ *Vav-Cre* mice were analyzed for Ca^{2+} influx (**g**) and activation of the NLRP3 (**h, i**) and NLRC4 (**h**) inflammasomes as described in panels b, c and f above. Ca^{2+} traces are representative of 2 repeat experiments; bar graphs show the mean ± SEM from 5 individual mice per group. Statistical significance was calculated with an unpaired Student's t test: **, $p<0.005$; ***, $p<0.001$.

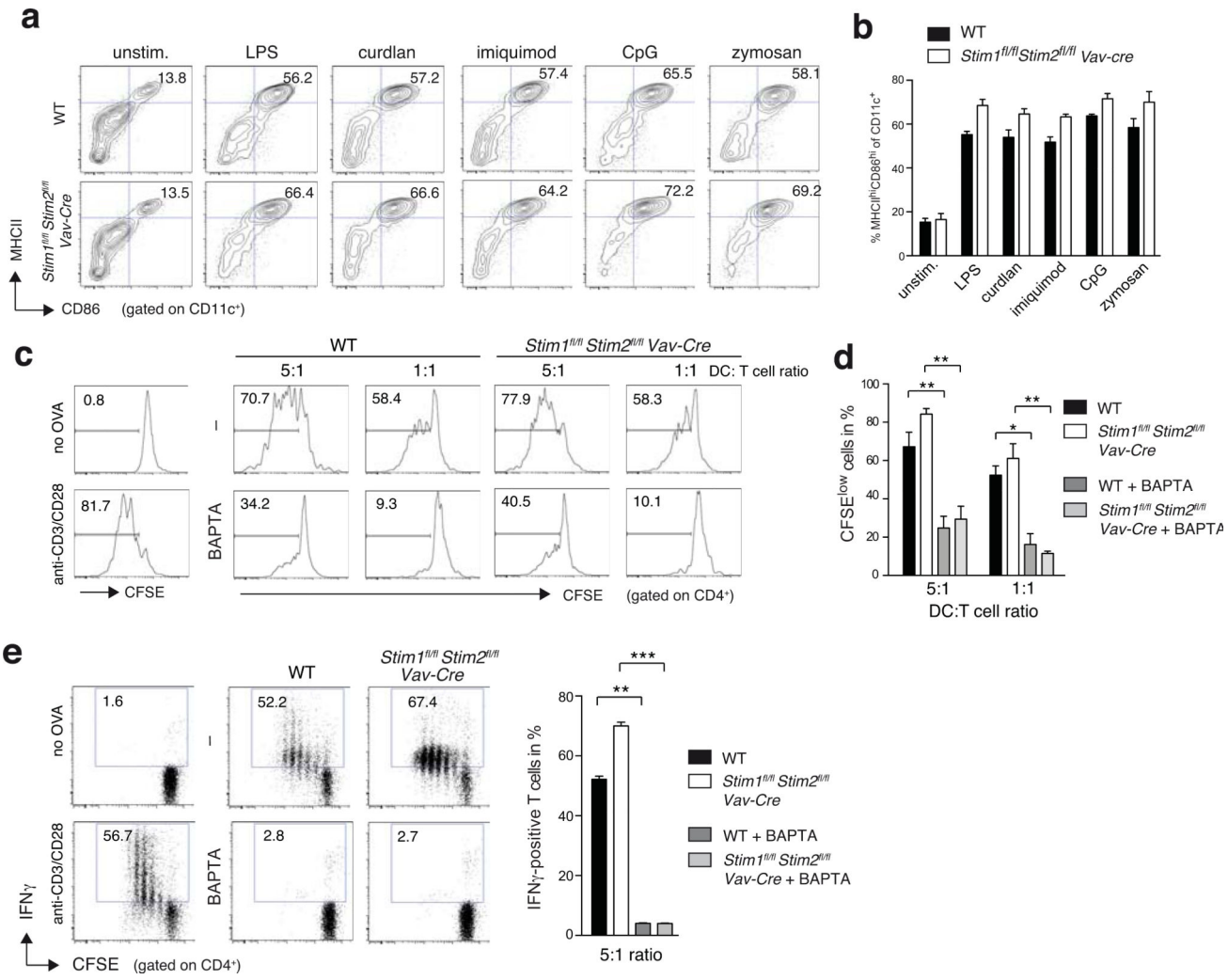

Figure 7. Antigen presentation by BMDCs and their ability to activate T cells is independent of STIM1 and STIM2

(a,b) Maturation of BMDCs does not require SOCE. WT and *Stim1$^{fl/fl}$Stim2$^{fl/fl}$ Vav-Cre* BMDCs were left untreated (unstim.) or stimulated with 1 μg/ml LPS, 50 μg/ml curdlan, 1 μg/ml imiquimod, 100 nM CpG, or 25 μg/ml zymosan for 16 h and expression of MHCII and CD86 on CD11c^{+} BMDCs was measured by flow cytometry. One representative experiment **(a)** and mean ± SEM of averaged frequencies of MHCII^{hi} CD86^{hi} BMDCs from 5 individual experiments **(b)**. **(c-e)** Antigen presentation and T cell activation by BMDCs. WT and *Stim1$^{fl/fl}$Stim2$^{fl/fl}$ Vav-Cre* BMDCs were maturated with 0.1 μg/ml LPS and incubated with 500 μg/ml OVA protein with or without 10 μM BAPTA-AM for 30 min. After washing, OVA-loaded BMDCs were co-cultured at 5:1 and 1:1 ratios with CFSE-labeled WT OT-II CD4^{+} T cells for 3 d before CFSE-dilution of CD4^{+} T cells was analyzed by flow cytometry. CFSE-labeled OT-II T cells were incubated with BMDCs without OVA protein (no OVA) or anti-CD3 and anti-CD28 mAbs (anti-CD3/28) as negative and positive controls, respectively. (**c,d**) Representative histogram plots **(c)** of proliferated CFSE^{lo} OT-II cells at different DC:T cell ratios and quantification (mean ± SEM) of 3 experiments **(d)**. **(e)** IFNγ production by OT-II cells was measured after co-culture of BMDCs and CFSE-labeled

OT-II cells at a 5:1 ratio for 72 h followed by restimulation with PMA plus ionomycin for 6 h in the presence of Brefeldin A. IFNγ was measured by intracellular cytokine staining (left panel); the frequencies of $IFN\gamma^+$ cells from 3 experiments are shown as mean ± SEM (right panel). OT-II T cells incubated with BMDCs without OVA protein (no OVA) or stimulated with anti-CD3 and anti-CD28 mAbs (anti-CD3/28) in the presence of 20 ng/ml rIL-12 were used as negative and positive controls, respectively. Statistical significance was calculated with an unpaired Student's t test: *, $p<0.05$; **, $p<0.005$; ***, $p<0.001$.

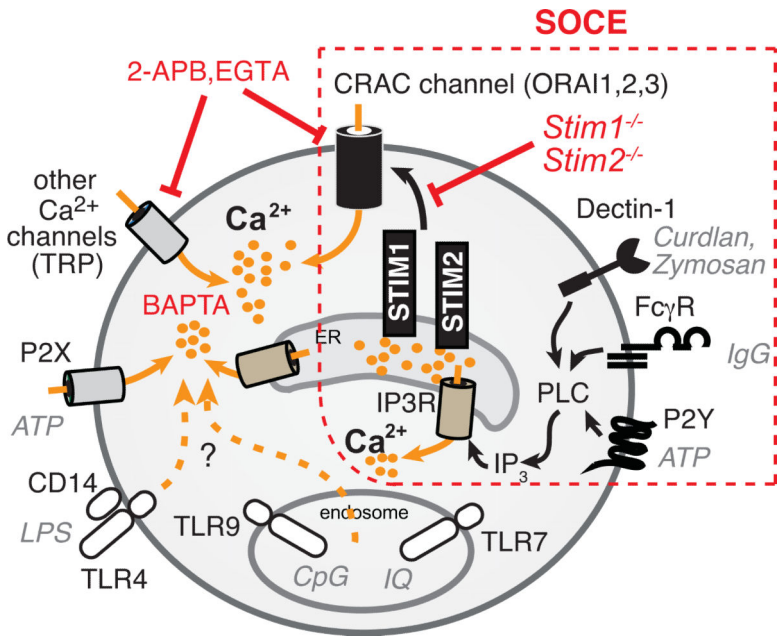

Figure 8. Intracellular Ca^{2+} signals but not SOCE regulate macrophage and DC function

Engagement of FcγR by IgG and Dectin-1 by zymosan or curdlan was shown to result in phospholipase C-mediated production of IP_3, which binds to and facilitates opening of IP_3R channels in the membrane of the ER. The resulting Ca^{2+} release from ER stores activates STIM1 and STIM2 located in the ER membrane and causes the opening of CRAC channels (ORAI1, 2 and/or 3) in the plasma membrane resulting in SOCE. Cells lacking STIM1/STIM2 have a selective defect in SOCE. Engagement of various pattern-recognition receptors (PRRs) such as TLR7 (by imiquimod), TLR9 (by CpG) and TLR4/CD14 (by LPS) was also reported to induce Ca^{2+} signals, although the channels that mediate these signals are unknown. Transient receptor potential (TRP) channels and P2X receptors contribute to Ca^{2+} influx in macrophages and DCs but are not store operated. EGTA chelates extracellular Ca^{2+} and prevents SOCE via CRAC channels and Ca^{2+} influx via other channels in the PM. 2-APB is a non-selective modulator of several ion channels in the PM and IP_3Rs in the ER. BAPTA-AM chelates all cytosolic Ca^{2+} and thereby neutralizes the effects of Ca^{2+} release from ER stores and extracellular Ca^{2+} influx.